

Spokesman: Kenneth K. Young
FTS No. 392-4186
Telephone: (206) 543-4186

Hadron Distributions in High P_t Collisions in a Very
Large Acceptance Calorimeter
(VLAC)

January 25, 1978

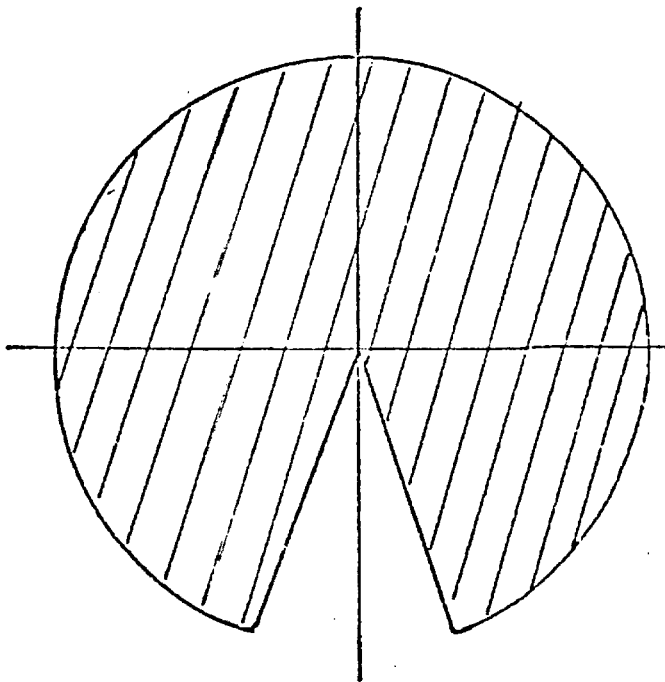
R. Carlini, V. Cook, P. M. Mockett, J. Rothberg, J. Rutherford

R. W. Williams, and K. K. Young

University of Washington

P. Mantsch and S. Pruss

Fermilab



44 pgs.

Summary for the VLAC Proposal

A. Physics Objectives.

In a high energy hadron collision which produces a high transverse momentum jet, we propose to map the hadron momentum distributions in a large part of the available phase space. The purpose of the maps is to:

(1) Measure the scattering contributions from quark-quark scattering, quark-gluon scattering and gluon-gluon scattering, by measuring the jet momenta, the width of the jets and their correlations.

(2) Measure the momentum distribution of the hadrons in the underlying soft P_t cloud.

(3) Measure the momentum distributions of the partons within the original hadrons by observing the momentum distributions normal to the reaction plane and by the angular correlations of the jet-jet interactions.

(4) Explore the structure function of hadrons by measuring the jets as a function of incident particle type.

(5) Explore the space time character of the cascading partons by measuring the jet characteristics as a function of the nuclear size by measuring the jet width and the changes in the jet-jet angular correlations.

B. Proposed Experimental Technique.

We propose to use a sampling lead-scintillator, and iron-scintillator segmented calorimeters to measure the vector momenta of the hadrons. This will be supplemented by tracking from multi-wire proportional chambers and spot detectors enclosed in the calorimeter. The apparatus will have an acceptance of more than four units of rapidity and the full azimuth for most of the rapidity range. The apparatus will be a much larger and improved version of the calorimeter type used in E236. We propose to use the hadron beam M1 or M2.

C. Duration of Time Required for Testing and Data Taking.

We estimate that a total run of 1200 hours will be sufficient for this proposal. About 200 hours will be required for testing. We estimate that 1000 hours of data taking will be sufficient for obtaining good data up to $P_t = 8$ GeV/c for several incident energies.

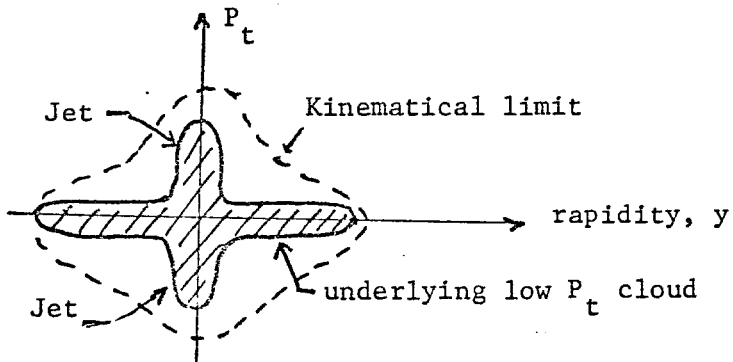
25 January, 1978

University of Washington and Fermilab

Introduction

We propose to measure the jet-jet correlations in high P_t energy collisions which are triggered by high P_t jets. We are motivated to design an experiment which has a very large acceptance by the hadron correlation results from the ISR large acceptance magnetic spectrometer measurements. The large acceptance will also benefit the measurement of the low P_t cloud that will accompany the high P_t jets in hadron-hadron collisions.

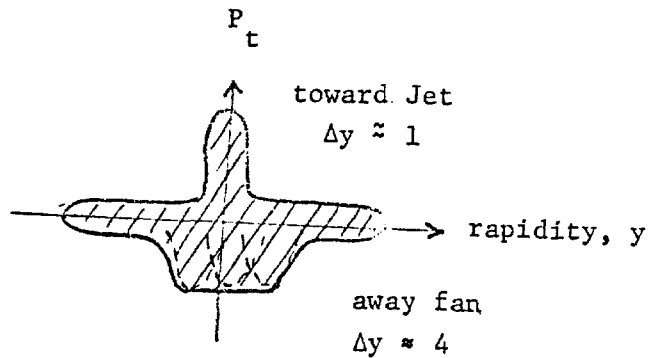
We are guided by the quark model that interprets these high P_t jet production events as the hard scattering of quark constituents. The hard scattered quarks fragment into large P_t hadron jets while the remaining spectator quarks in the original hadrons fragment into the underlying low P_t cloud. This is shown symbolically in a phase space diagram below.



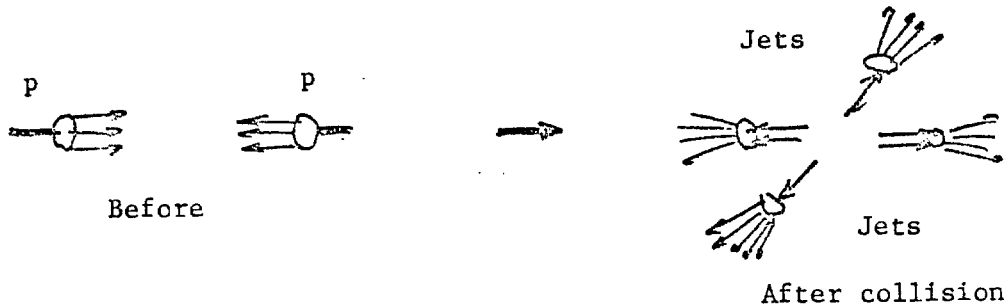
Recent interpretation of the available data favor the inclusion of quark-gluon scattering as well as quark-quark scattering as necessary to be consistent with the data. If we are to understand the dynamics at the modest P_t 's available at Fermilab, we will need to measure the details of the possible quark jets as well as gluon jets.

Results from the large solid angle spectrometer experiments at the ISR and elsewhere have indicated a jet-jet structure in events which have been

triggered by a high P_t particle or a high P_t jet. The ISR results are particularly informative because of their large acceptance. The two jets which are produced in a high P_t collision are not well correlated in angle. A sum over many events with a fixed angle high P_t trigger show a narrow correlation in the side "toward" the trigger. The away side, however, has quite a wide correlation width. The data of Della Negra, et al., illustrate this in Figure 1. The ISR experimenters have characterized the observed distributions as having a "toward jet" and an "away fan". The characteristics of this are shown in the figure below:



The characteristic of the "toward jet" is 1 unit of rapidity while the "away fan" is characterized by a width of 4 units of rapidity. The underlying low P_t cloud has not been measured in high P_t jet experiments. Note that the "away fan" is an artifact of the compilation of many events. Each event is characterized by a jet-jet structure, but the "away jet" has a wide correlation width with respect to the "toward jet". We expect that the low P_t cloud should be just forward, and backward jets produced by the forward and backward spectator partons and the "wee partons".



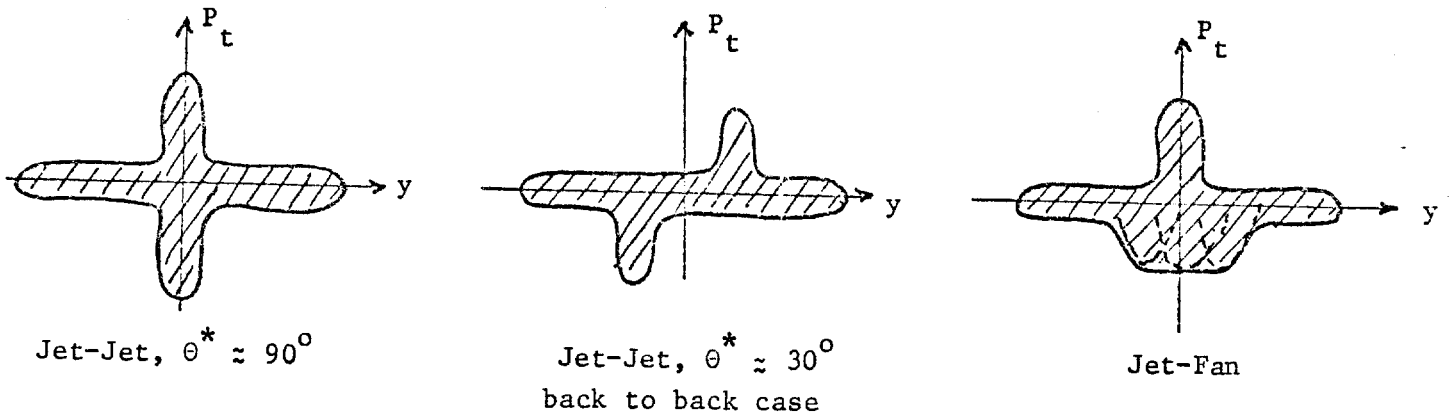
The existence of the underlying low P_t cloud has complicated the interpretation of the jets and fans because we do not know whether any given hadron belongs in the jet or in the cloud. Measurements with modest acceptance do not allow a reliable extrapolation of the low P_t cloud to make an unambiguous definition of the jet.

Structure Functions of the Hadrons.

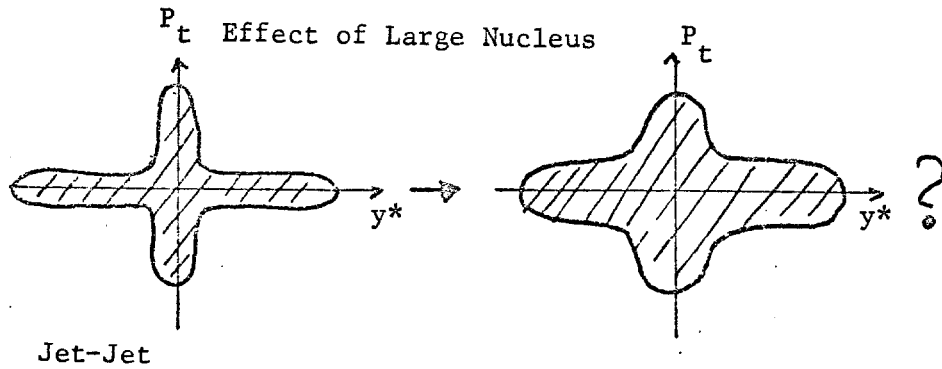
The large azimuthal acceptance of the VLAC permits a study of the hadron and jet distributions transverse to the reaction plane (defined by the jet and beam axes) in a way which has minimal geometrical bias. This study will provide a tool for the understanding of the momentum distributions of the quarks in the hadrons.

Minimum requirements for the next generation experiment.

It has become clear that a study of these high P_t events with a large acceptance device which will find the hadron distributions in all of the phase space will greatly advance the understanding of the underlying physics. When the whole phase space is observed, the experimenter can see enough to separate the contributions of the low P_t underlying cloud from the jets over a large angular range.



The hadron distribution variation with the size of the target nucleus will likely prove to be very useful tool in obtaining an understanding of the scattering of partons which must emerge from the sea of nuclear matter in heavy nuclei. Perhaps the hadron distributions grow wider in momentum space.



In summary, we propose to map out the hadron momentum distributions in a large part of the available phase space for large P_t collisions at all available energies. The purpose of the maps is to:

(1) Measure the scattering contributions from quark-quark scattering, quark-gluon scattering, and gluon-gluon scattering, by measuring the jets, the width of the jets and their correlations.

(2) Measure the momentum distribution of the hadrons in the underlying soft P_t cloud.

(3) Measure the momentum distributions of the partons within the original hadrons by observing the momentum distributions normal to the reaction plane and by the angular correlations of the jet-jet interactions.

(4) Explore the structure function of hadrons by measuring the jets as a function of incident particle type.

(5) Explore the space time character of the cascading partons into hadrons by observing the jet characteristics as a function of the nuclear size by measuring the jet width and the changes in the jet-jet angular correlations.

Proposed Detector

We propose to build a very large solid angle device that will measure all of the necessary phase space excluding the backward jet. The device is a dense calorimeter which has good energy and spatial resolution. The good spatial resolution allows the calorimeter to be placed at a modest distance from the target to obtain the necessary angular resolution. The total size of the calorimeter then can be made with dimensions that are compatible with straight-forward, proven, technology. Figure 4 shows the layout of the proposed calorimeter. The polar angle acceptance is shown in Figure 7.

The front section of the calorimeter will be a segmented electromagnetic shower detector of sufficient depth to separate the contributions from photons, electrons, and hadrons. The design of the calorimeter has been proven in E236. With this compact design, the r.m.s. energy resolution is $(51\sqrt{E} + 4)\%$ and the r.m.s. spatial resolution is 0.5". The calorimeter segmentation into horizontal and vertical strips has been successfully

exploited in E236 to obtain good measurements of the projected energy distributions of the incident hadrons.¹ The replication of the E236 calorimeter in larger form will allow us to pursue the physics stated in the previous section. However, in the present proposal, we have improved the design so that the two-dimensional distributions can be obtained rather than just the projected distributions. This will be accomplished by: (a) Using horizontal and vertical scintillators in the same gap in the steel so that the pulse height signature will be much less ambiguous in the corresponding x-y strips; (b) addition of "spot chambers" for direct two-dimensional information. These spot chambers will be proportional wire chambers with readout spots of coarse resolution.

The tracking of the charged particles and the selection of events which originate in the target will be obtained from the PWC's between the liquid hydrogen target and the calorimeter.

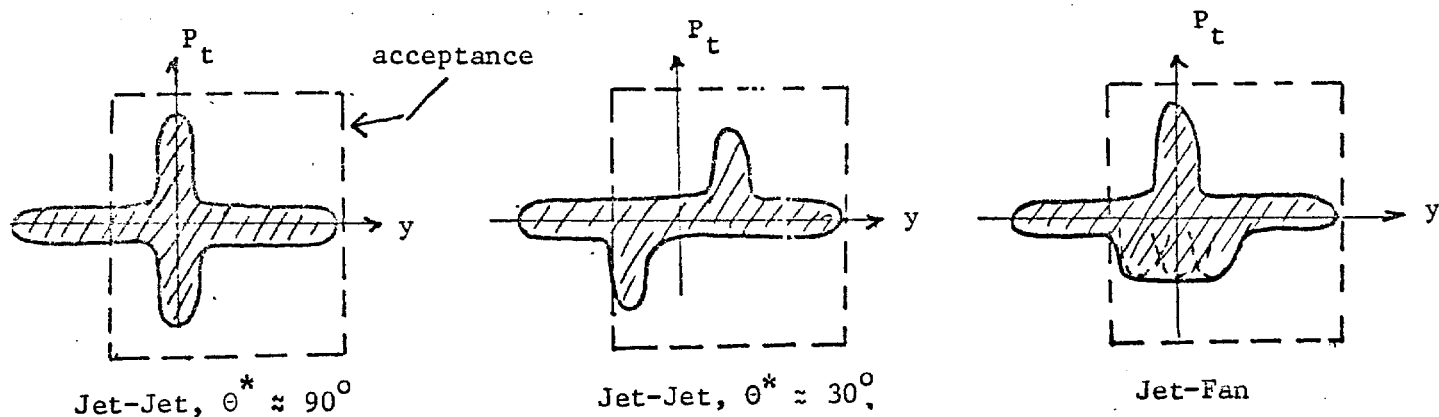
The Trigger

As in E236, we will combine the weighted sum of pulse heights from the calorimeters on each side to produce a threshold in P_t for the trigger. Also we will provide the ability to trigger on single particles with large P_t in order to provide a good systematic normalization of jets to single-particle cross sections.

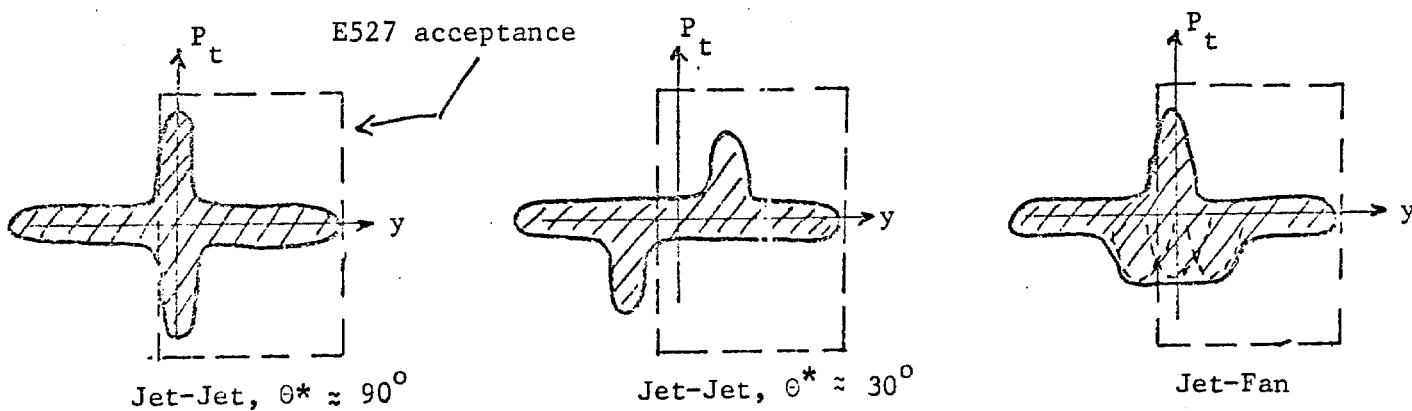
In E236 we found that the largest P_t triggers were dominated by reactions

upstream that were not vetoed by the anti-shield upstream of the target. In this experiment, we will use a multi-layer anti-shield and dE/dx for the beam counter to assure much higher vetoing efficiency for upstream interactions. With these improvements, we will be able to take larger beam rates without being limited by the dead time of the apparatus caused by the upstream interactions.

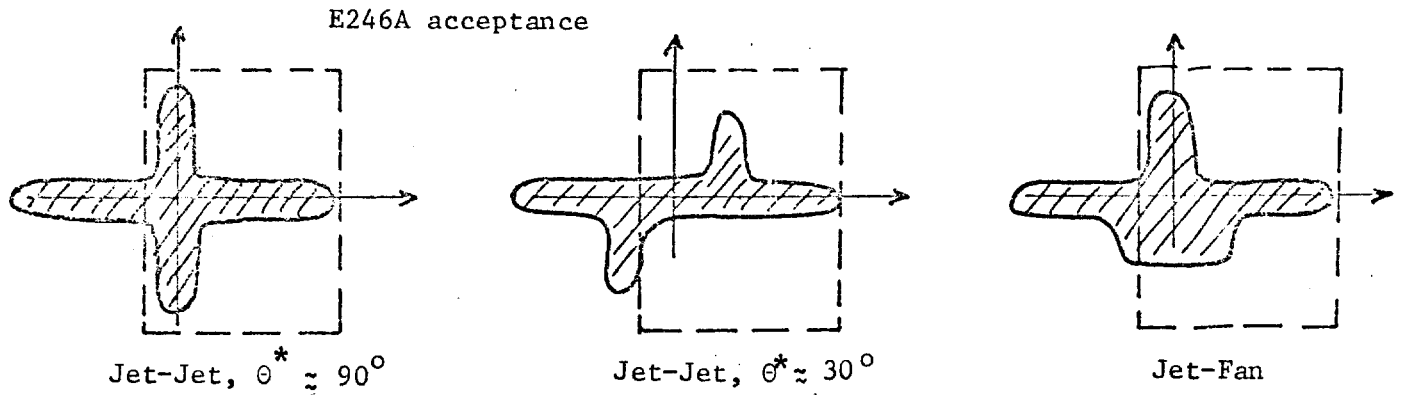
Our proposal will be able to make the measurement of the hadron distribution with the acceptance shown below:



For comparison purposes, the approved experiment E527 has the following acceptance.



Proposal E246A has the following acceptance:



A table of comparison for the calorimeters is shown in the following

Table:

Comparison Chart for Next-Generation Jet Experiments

(Assume $P_{in} = 400$ GeV)

	<u>527</u>	<u>246A</u>	<u>This proposal</u>	<u>Desiderata</u>
cms acceptance at 400 GeV.				
Min. rapidity, y^*	-.42	-1.0	-1.9	-2
Max. rapidity, y^*	3.4	3.4	3.4	3.4
calorimeter energy resolution.	$89\%/\sqrt{E}$	$89\%/\sqrt{E}$	$(51/\sqrt{E} + 4)\%$	
segmentation rapidity interval at $y^* = 1$	0.7	0.7	0.28	0.2
rapidity interval at $y^* = -.4$.15	.26	.20	0.2
Spatial resolution			0.5 in.	
Azimuthal Acceptance at $y^* = -1$ on one side		$\pm 47^\circ$	$\pm 90^\circ$	$\pm 90^\circ$

The approved experiment E527 would have the possibility of mapping the jet-jet interactions for jets near $\theta^* = 90^\circ$. It will not be capable of systematically measuring the large angle jet-jet correlations nor will it be able to map the events which have a jet and fan in the final state. This proposal will have a

sufficiently large acceptance and sufficient resolution in both energy and space to make good measurements on a large class of events with large P_t . This includes jets at large angles. The high speed PWC and data logging system which we have proven in E236 and E439 will allow us to utilize high intensity beams so that we will be able to obtain significant data up to 9 GeV/c for normal amounts of running time.

Measurements obtainable with the VLAC

A straight-forward approach to the measurement of the hadron distributions is to measure the vector momentum of each particle emitted in the collision. The clustering of the particles in the toward and away jets and the forward and backward jets allow the parametrization of the event by the 4 or more jet axes. The measurement of the vector momenta of the jets, interpreted as the final vector momenta of the partons involved in the collision, obtains a view of the dynamics of parton scattering via the strong interaction. The clustering of the individual particles about the jet axes characterizes the parton cascade into hadrons. This has been measured and found to be similar to the jets produced at SPEAR and in deep inelastic lepton scattering. Unfortunately, no experiment at the Fermilab or CERN has yet been devised which follows the above procedure for high P_t jet triggers. Limitations may include too little acceptance and lack of neutral particle measurements.

Using the calorimeter approach of VLAC, we have chosen a method which is complementary to the limitations of spectrometer measurements. With VLAC, we will be able to measure the vector momenta of the jet axes with good accuracy (including both charged and neutral particles) over a large

kinematical region. This has a direct interpretation for quark scattering dynamics and the distribution of the quarks before the collision (fermi motion).

We will be able to characterize the hadron distributions about the jet axes by examining the width of the energy deposition about the jet axis. This integral distribution can be interpreted using a model of the parton cascade. We have done this in E236 to show that the jets observed are consistent with the SPEAR jets. Figure 3 shows the characteristic energy deposition about the jet axis for a number of events. The width of the jet for an individual event can be obtained by calculating an r.m.s. width for each event. This method is amenable for differentiating between SPEAR-like jets (quark jets) from the possibly different jets which may result from the jet produced by gluons.

Single particle measurements

Measurements of single particle production will be made in VLAC for particles produced in the backward hemisphere. The folding of particles in the forward direction will make it difficult to distinguish individual particles in the forward direction. The VLAC has circles of confusion for the separation of individual particles which are small for photons but which are 2" in diameter for the hadrons which shower in the steel calorimeter. The energy deposition for a single particle is shown in Figure 3. The ability, then to examine the single particle inclusive distributions about the jet axes is restricted to the photons and to a limited region of phase space for the hadrons. Figure 2 shows the diameters of the circles of confusion for the separation of pairs of hadrons. It is mostly in the backward hemisphere that the separation of individual hadrons will be possible.

To summarize, VLAC will be able to make good measurements of jet vector momenta over a very large solid angle. In the same kinematical region, VLAC will be able to characterize the jet by the integral energy distribution. Over a restricted phase space, VLAC will be able to make good measurements of the single particle inclusive distributions. The character of the measurements here will be qualitatively different from those obtained with devices which have smaller acceptance. We will be able to characterize each event with the vector momenta of the jets which are close to the basic dynamics of parton scattering. The small acceptance experiments often will only be able to measure the statistical distributions of many events which is one step removed from the above procedure.

Details of the Calorimeter

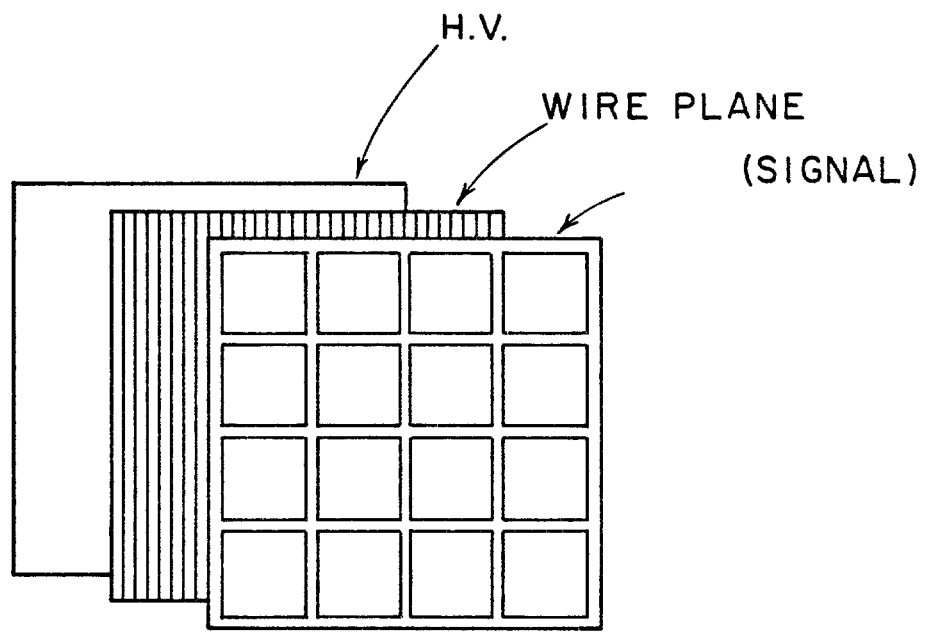
The apparatus consists of five groups of MWPC's and 3 segmented calorimeters as shown in Figures 4 and 5. The cms polar angle acceptance is shown in Figure 7. There are 3 sets of "spot detectors" associated with the apparatus. The detectors are embedded in the calorimeter itself as indicated in Figure 6. These remove ambiguities in x-y position correlations that occur if only x-y scintillation detectors are used as in the E236 calorimeter.

Spot Detectors

Multiwire proportional chambers or drift chambers could be used as spot detectors to provide two-dimensional position information with coarse resolution. One approach would involve a two-dimensional array of rectangular readout "spots" in a plane parallel to the proportional chamber wires. A

pulse induced on these "spots" by the development of a nearby avalanche would be amplified and read out into a register. We understand that similar devices have been used at SLAC for a hodoscope. There are variations on this which could prove convenient and less costly; one alternative would be to use drift cells to define one coordinate. A delay line situated close to the sense wire in each cell would provide information on the second coordinate. This mode of operation considerably reduces the number of electronics channels required. There is no ambiguity even for multi-hit events since the travel time on the delay line is measured independently of the drift time. Our group has experimented with similar drift chambers with delay line readout. We have worked with flat zig-zag etched lines and rather wide drift cells. The resolution requirements for these spot detectors are much less severe than usual. We have also designed and constructed a 16-hit digitizer system for drift chambers which would be very suitable for this application. The time resolution and the multi-hit capability seem well matched. Since the width of the drift cells will vary with angle, the expected number of hits per cell should be well below 16. In the forward direction where the rates are high and accidentals could be a problem, we would use spot detectors with suitably small spots.

The cost of readout electronics for the delay lines is about \$30 per channel and the cost of the delay line itself averages to about \$50 per channel. Assuming a total cost of \$150 per channel and 100 channels (a modest-sized system) the total cost is \$15,000. The spot detector approach would require perhaps as many as 3,000 channels (still not a large PC system; our E236 system has 14,000 wires) at about \$10 per channel for a



Spot detector with coarse spot readout

system cost of \$30,000. This cost does not include the computer readout system and the fabrication of the chambers which would be similar for any design.

The new calorimeter system provides a solid coverage in theta of 30° in the lab. This corresponds to a rapidity interval of 4 units. Unlike the E236 calorimeters the vertical scintillators in both the lead and iron sections would be divided into units of constant rapidity (.2 units/interval). The center calorimeter would have segmentation not smaller than 1" ($.58^\circ$ in the lab) and have only up and down tubes but will use timing to obtain vertical position information.

The calorimeter segments are tapered so that the angle subtended by each segment from the target is approximately constant. We have found in E236 that this feature is important for the purpose of preserving the angular information of the hadron shower in a calorimeter that does not have longitudinal segmentation. In the direction where the hadron showers cross boundaries of segments, the variation in the longitudinal development of showers will cause a loss of angular resolution. In E236, we found that the tapered segments produced a r.m.s. deviation of the calorimeter-determined particle position from the true particle position of 0.5". Figure 8 shows the average position distribution. The energy deposition spread of a single hadron incident on the calorimeter is shown in Figure 3. We interpret this to mean that the circle of confusion for separating a pair of particles incident on the calorimeter to be 5 cm in diameter at the 60% level.

The energy resolution of the calorimeter for this experiment should be identical to that obtained by the E236 calorimeter. Figure 9 shows the

spread of energy measured for a monoenergetic hadron beam incident on the calorimeter. Figure 10 shows the change in resolution as a function of hadron energy, which is parameterized as $\frac{\Delta E}{E}(\text{FWHM}) = \frac{1.2}{\sqrt{E}} + 0.09$ or $\frac{\sigma}{E} = \frac{0.51}{\sqrt{E}} + .04$. The linearity of the calorimeter, shown in Figure 11, is good to 2%.

Table 1 along with Figures 4, 5, and 6 give the mechanical specifications of the calorimeter system.

The results of Monte-Carlo calculations are superimposed on the beam's eye view of the calorimeter in Figure 12a through 12c. The Monte Carlo generates a SPEAR-type jet in the center-of-mass system and transforms the distributions into the lab and projects them to the front face of the calorimeter. The θ angular distributions are those for single particles. These indicate that the mechanical dimensions of the calorimeter are sufficient to observe such jet events.

How the various types of jet-jet events will look on the calorimeter.

In Figures 14a to d we show how events with various distributions in "rapidity - P_t " space would be projected on the calorimeter. The forward jet would be concentrated around the beam while the backward jet would be a dilute distribution over the entire face of the calorimeter.

TABLE 1 - CALORIMETER

Nominal Position:	102" from the target	
Angular Acceptance in the Laboratory:	Horizontal: $\pm 30^\circ$	
	<u>Electromagnetic Detector</u>	<u>Hadronic Detector</u>
Interaction Material/Detector	Lead/Scintillator	Iron/Scintillator
Segmentation	<u>Toward+Away</u>	<u>Toward+Away</u>
	Vertical strips: 24 segments (.2 units of rapidity outer segments)	Vertical strips: 24 segments (.2 units of rapidity outer segments)
	Horiz. strips: 56 segments (.2 units of rapidity outer segments) (.58 $^\circ$ per segment inner segments)	Horiz. strips: 56 segments (.2 units of rapidity outer segments) (.58 $^\circ$ per segment inner segments)
	<u>Center</u>	<u>Center</u>
	Vertical strips: 20 segments (.58 $^\circ$ per segment)	Vertical strips: 20 segments (.58 $^\circ$ per segment)
	$\frac{1}{4}$ " Pb, $\frac{1}{4}$ " X-scintillator $\frac{1}{4}$ " Y-scintillator	1" Fe, $\frac{1}{4}$ " X-scintillator $\frac{1}{4}$ " Y-scintillator
Total Samples	16	64
Radiation/Collision Length	10.2 rad lengths	7.7 nuclear collision lengths
Total number of photomultiplier tubes	100	100
MASS	3 tons	47 tons

Changing the Configuration of the Calorimeters to Optimize Resolution.

Improved resolution in the forward hemisphere.

As seen in Figure 2a, the rapidity resolution of jets in the forward hemisphere (positive cms rapidity) is fair to poor when the calorimeter is in the 100" position. To improve the angular correlation of jet pairs with one jet emitted in the forward quadrant, we will want to move the toward calorimeter to the 200" position. The net rapidity resolution for the correlation is expected to be better than ± 0.14 for this configuration for rapidity < 1 . To obtain good angular resolution for two jets going into the forward hemisphere, we would put both calorimeters at the 100" position.

Trigger Rates and Background

The important rate to consider is the event rate at the highest P_t . The lower P_t trigger rates can be controlled by prescaling lower threshold triggers.

With modest improvements in the beam halo, we would expect that the background rate would be lower so that we would have a slight improvement in the E236 event rate. In E236 we have obtained an event rate for incident 340 GeV/protons of 2 events/GeV/hour at $P_t = 8$ GeV/c. The maximum beam rate was limited by the maximum charged particle rate in the PWC's. A sample of 1,000 events with a $P_t = 8$ GeV would take 500 hours to accumulate. For a 1,000 hour run with three beam energies, we would expect to accumulate data as follows:

No. of Events for a 1,000 Hour Run

<u>P_t</u>	<u>200 GeV</u>	<u>300 GeV</u>	<u>400 GeV</u>
8 GeV	90	800	1,000
3 to 8 GeV	10 ⁷	10 ⁷	10 ⁷

Run Request and Time Scale

We request a total of 1,200 hours for this experiment; 200 for testing and debugging, and 1,000 for data taking.

Assuming that the Meson Laboratory recovers from Mesopause in January, 1979, we can have our calorimeters ready for testing by that time. The PWC's and the data acquisition equipment and computer will be the same as that used in E236 and E439.

The M1 beam line with improved shielding for the halo would be quite suitable for this experiment. In E236, we were not able to reach 400 GeV because of problems with the magnets. Presumably, this situation will be more than corrected after the Mesopause. Since we will want to run with the highest momentum beams, including 1 TeV, we will be open to suggestions as to the optimum beam line. The beam intensity that we require is 3×10^6 particles/pulse which is not very stringent. The other requirements in order of preference are:

1. 200 GeV to 1 TeV
2. Cherenkov counters to count minority particles.
3. Exceptionally clean halo.

Costs

It would be suitable to use the PWC system, interfaces and computer system from E236, and the fast electronics from PREP. The additional cost will be in the materials and fabrication of the new calorimeters.

1. Iron

$$m = 47 \text{ mT}$$

$$\text{Iron cost} = 47 \text{ mT} \times \frac{\$.4\text{K}}{\text{mT}} = 19\text{K}$$

$$\text{Fabrication:} \qquad \qquad \qquad 19\text{K}$$

$$\text{Total:} \qquad \qquad \qquad \$38\text{K}$$

2. Lead

$$m = 3.2 \text{ mT}$$

$$\text{Cost} + 3.2 \text{ mT} \times \frac{\$2\text{K}}{\text{mT}} = \$6.4\text{K}$$

$$\text{Fabrication:} \qquad \qquad \qquad 6\text{K}$$

$$\text{Total:} \qquad \qquad \qquad \$12.4\text{K}$$

3. Scintillator

$$\text{Area} = 558 \text{ m}^2$$

$$\text{Cost: NE114 scintillators } (\$150/\text{m}^2) \times 558\text{m}^2 = \$84\text{K}$$

$$\text{Fabrication:} \qquad \qquad \qquad \$25\text{K}$$

$$\text{Total:} \qquad \qquad \qquad \$109\text{K}$$

4. Light Collectors

$$\text{Area} = 12\text{m}^2$$

$$\text{Cost: } 12 \times \$.6 = \$7.2\text{K}$$

5. PM tubes and bases

$$\text{Cost: } 200 \text{ tubes \& bases @ } \$200 = \$40\text{K}$$

6. Spot Chambers

Delay readout	\$15K
or	or
Individual readout	\$35K

7. Light flashers, etc. 5K

TOTAL COSTS:

Materials costs	\$156K
Fabrication costs	80K
	<hr/>
	<u>\$236K</u>

FIGURE CAPTIONS

1. Hadron distributions in the away and toward sites from Della Negra, et al., CERN/EP/PHYS 76-43, CERN.
2. (a) Resolution in rapidity as a function of rapidity. Note that the scales for cms rapidity at various target-to-calorimeter distances is also shown.
(b) Azimuthal angular resolution as a function of rapidity.
(c) Circle of resolution for single particles incident on the calorimeter as a function of rapidity. The resolution for the jet should be somewhat better than the single particle resolution.
(d) Circles of confusion for the separation of pairs of hadrons as a function of rapidity.
3. Energy clustering around the jet axes and for a single incident particle.
4. Detector layout, plan view .
5. Detector layout, front view.
6. Details of the hadron calorimeter.
7. Polar angle acceptance of the calorimeter.
8. Resolution in position for a single particle in hadron calorimeter.
9. Energy resolution for a single particle in the calorimeter.
10. Hadron energy resolution as a function of incident energy.

figure captions

11. Linearity of calorimeter as a function of incident energy.
12. (a) : Some examples of Monte Carlo jet-jet events superimposed on the calorimeter.
13. A Monte Carlo jet-jet event with circles of confusion on the beam's eye view of the calorimeter.
14. The clustering of jets for various types of events.(a to c)
15. Acceptance of E247A compared to VLAC.

From Della Negra, M. et al
 Preprint CERN/EP/PHYS 76-
 43, CERN

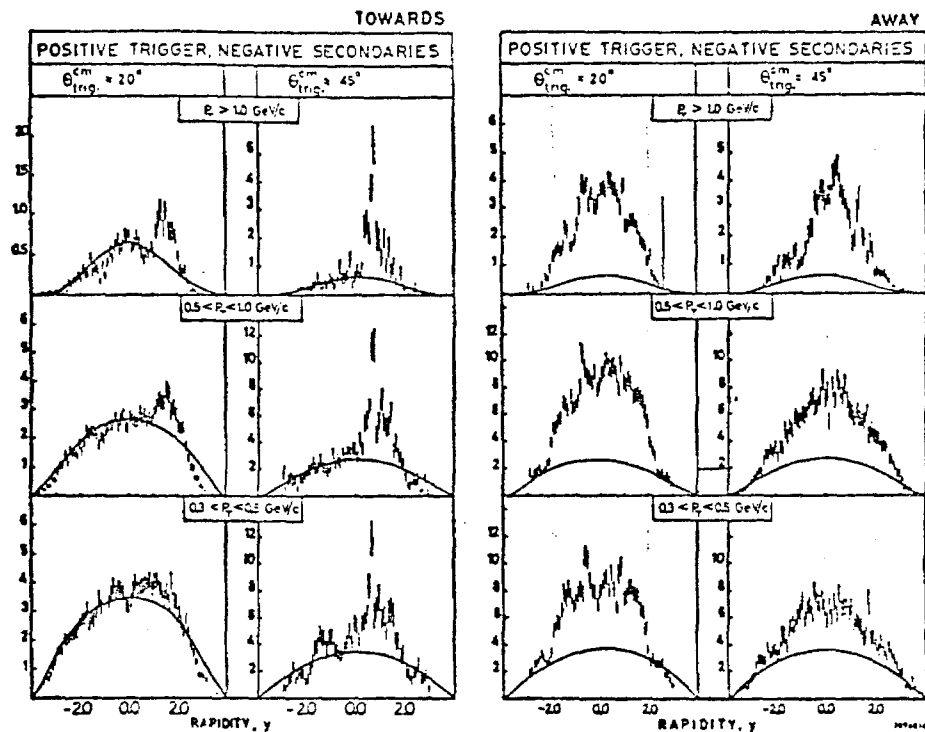


Figure 1.
 ——— normal event distribution

RESOLUTION OF CALORIMETER IN RAPIDITY
 AS A FUNCTION OF RAPIDITY
 ASSUME $P_{in} = 400 \text{ GeV}$

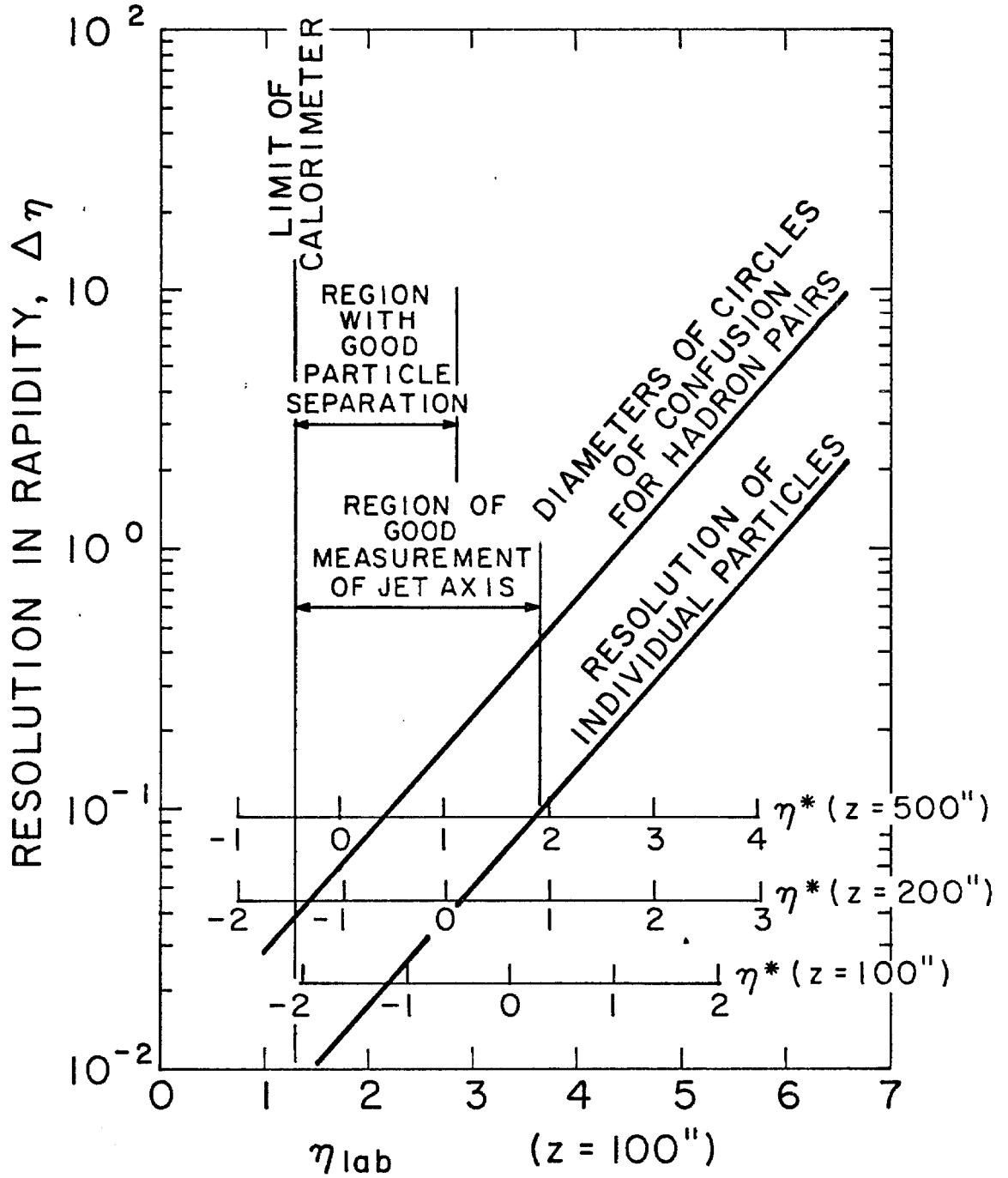


figure 2(a)

AZIMUTHAL ANGULAR RESOLUTION AS A FUNCTION OF RAPIDITY

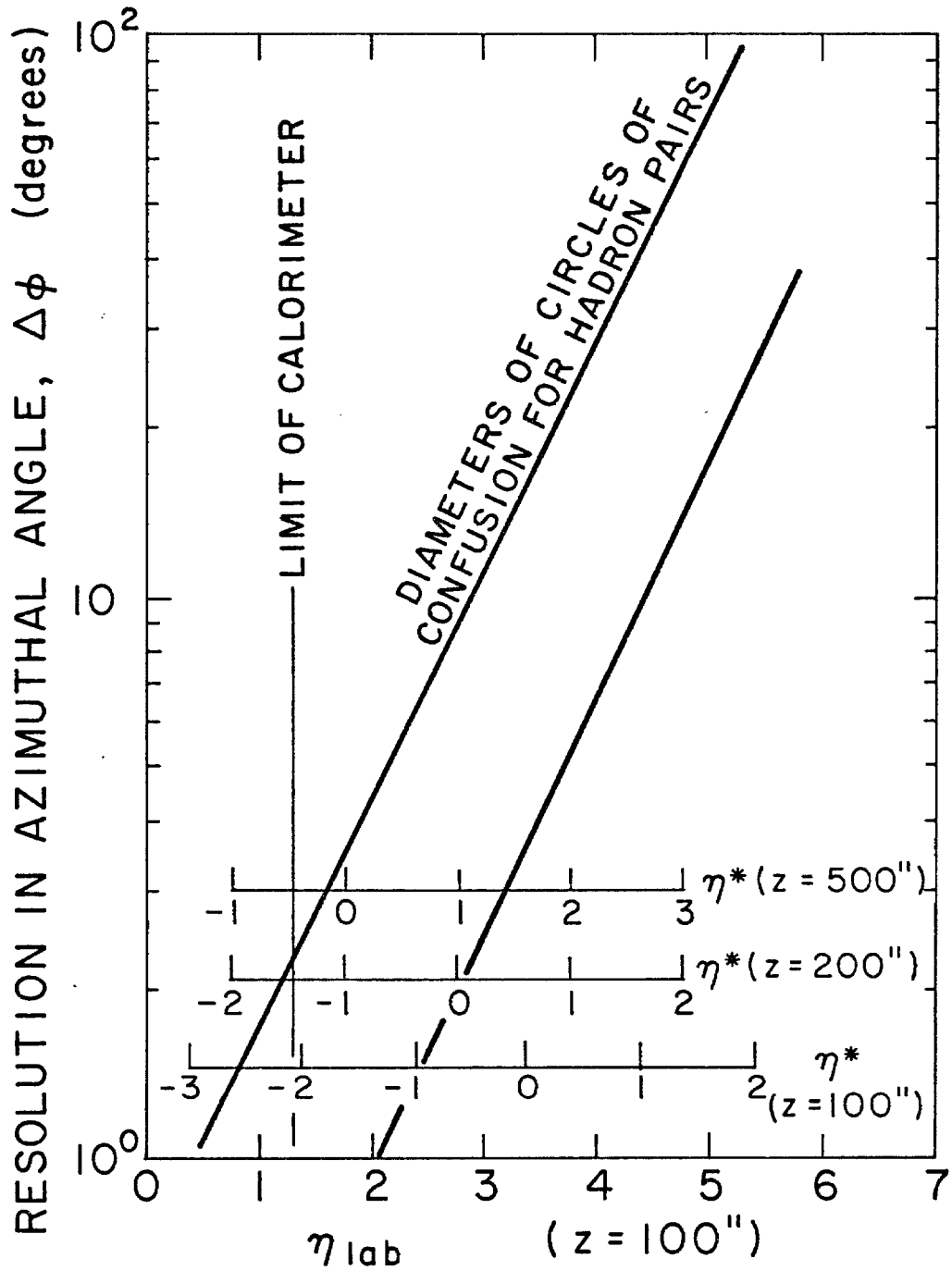


figure 2(b)

RESOLUTION FOR
 AXIS OF SINGLE PARTICLE

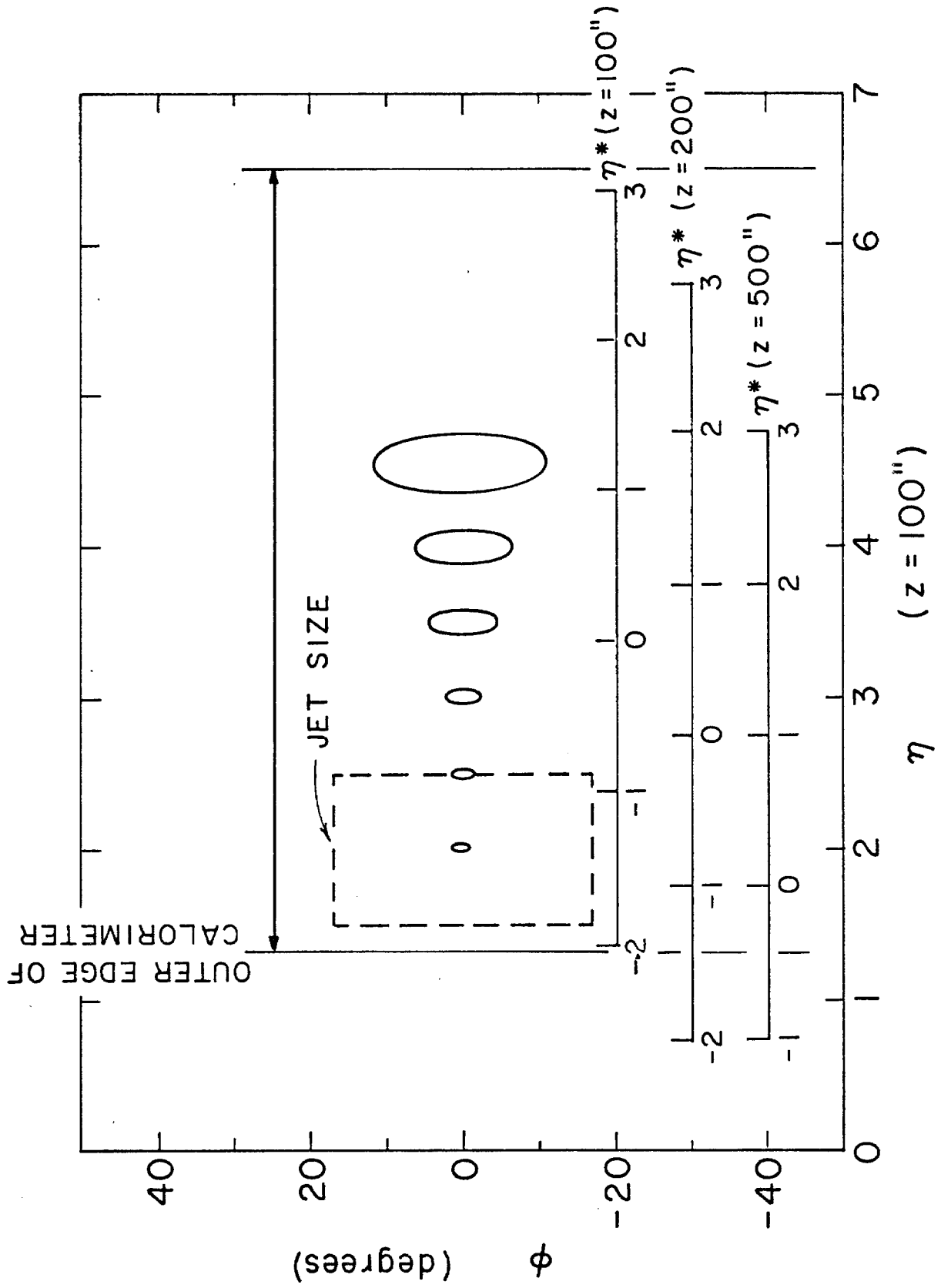


figure 2(c)

THE SIZES OF THE CIRCLES OF CONFUSION FOR SEPARATION OF PAIRS OF PARTICLES

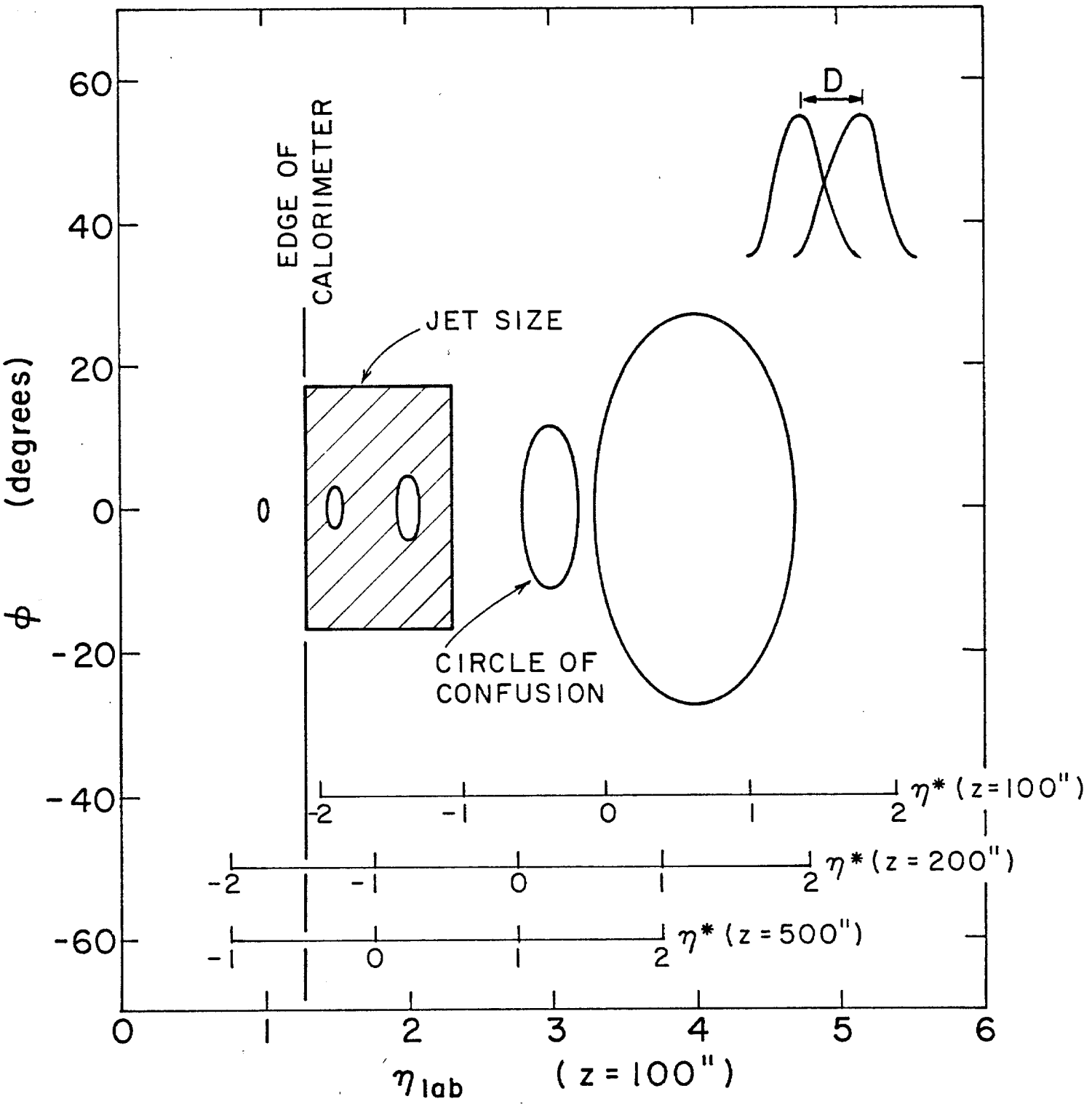


figure 2(d)

ENERGY CLUSTERING AROUND JET AXES

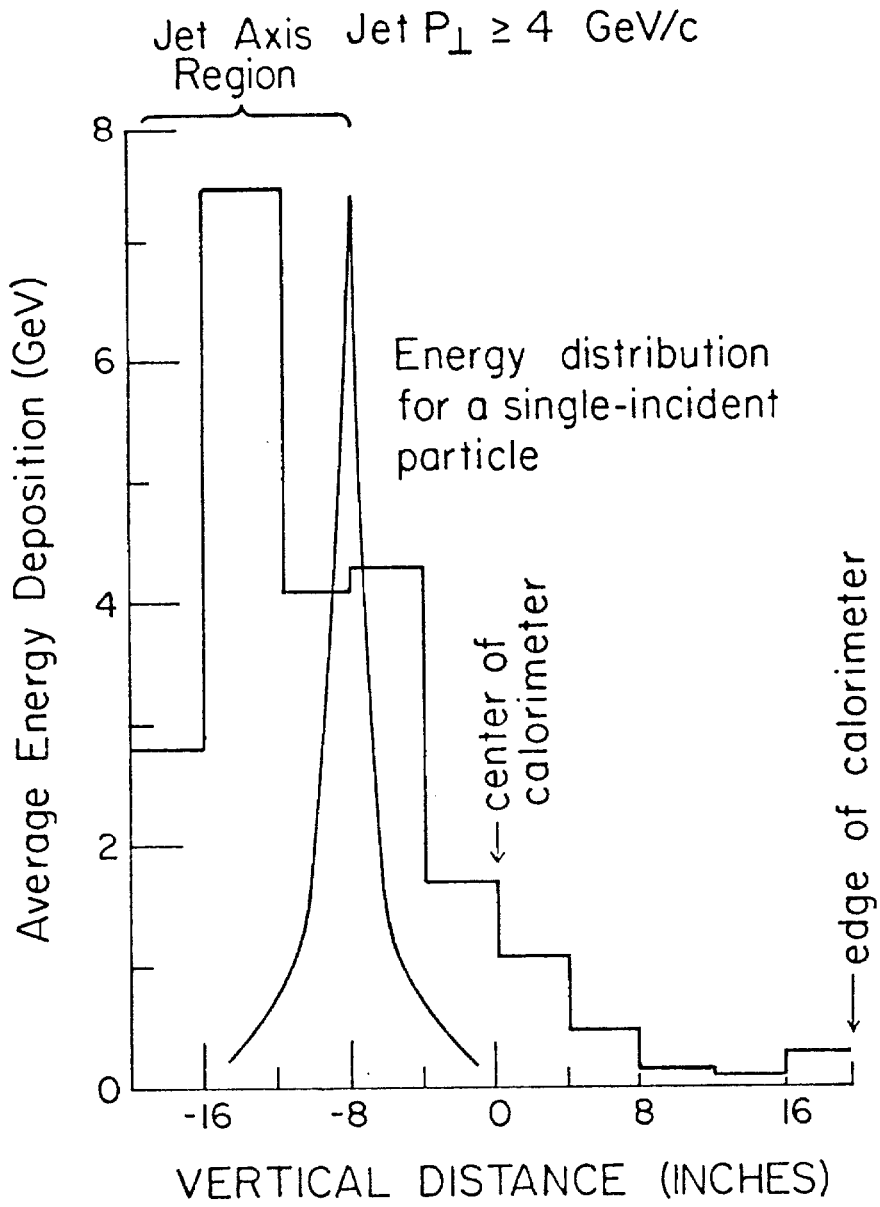


figure 3

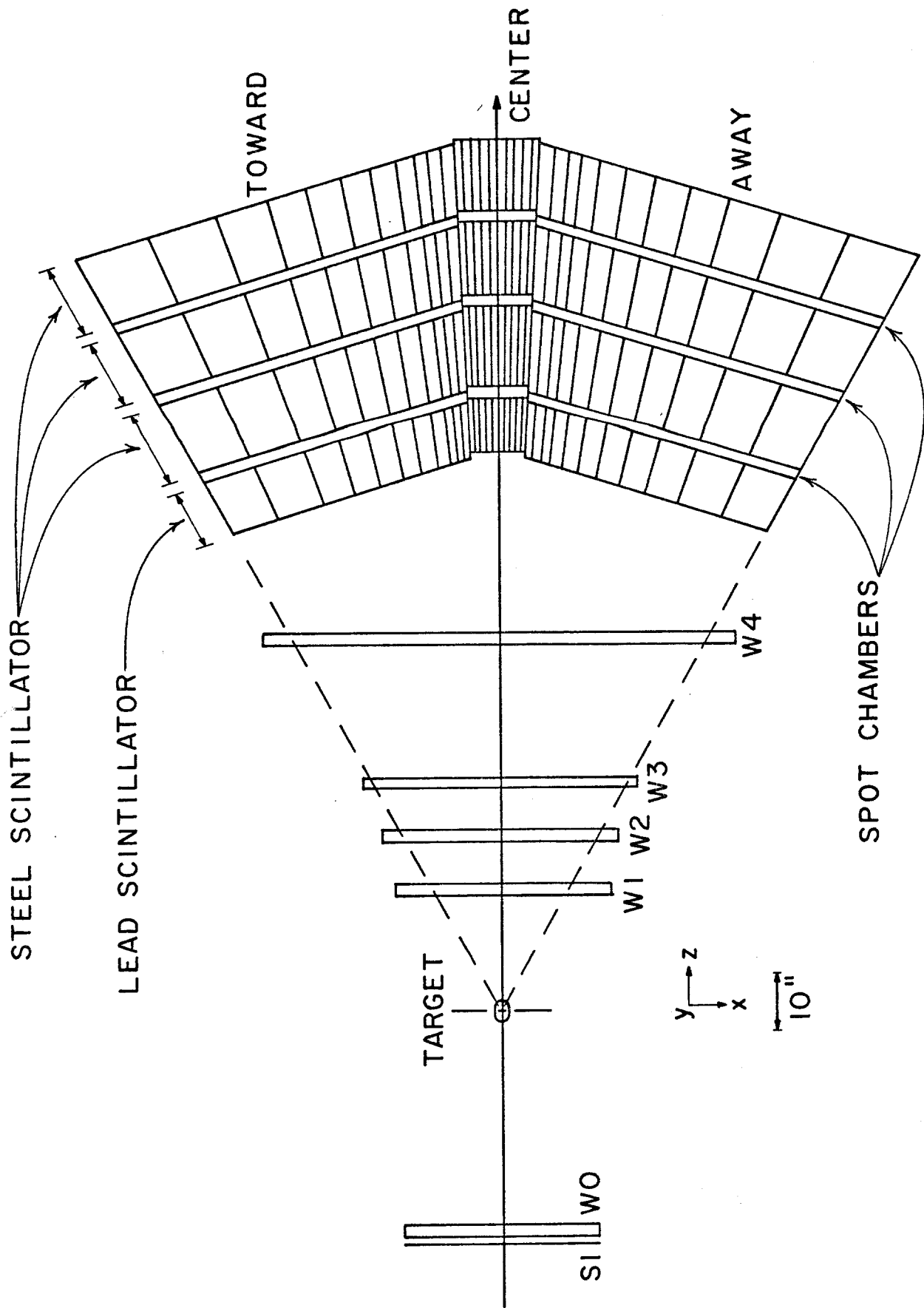
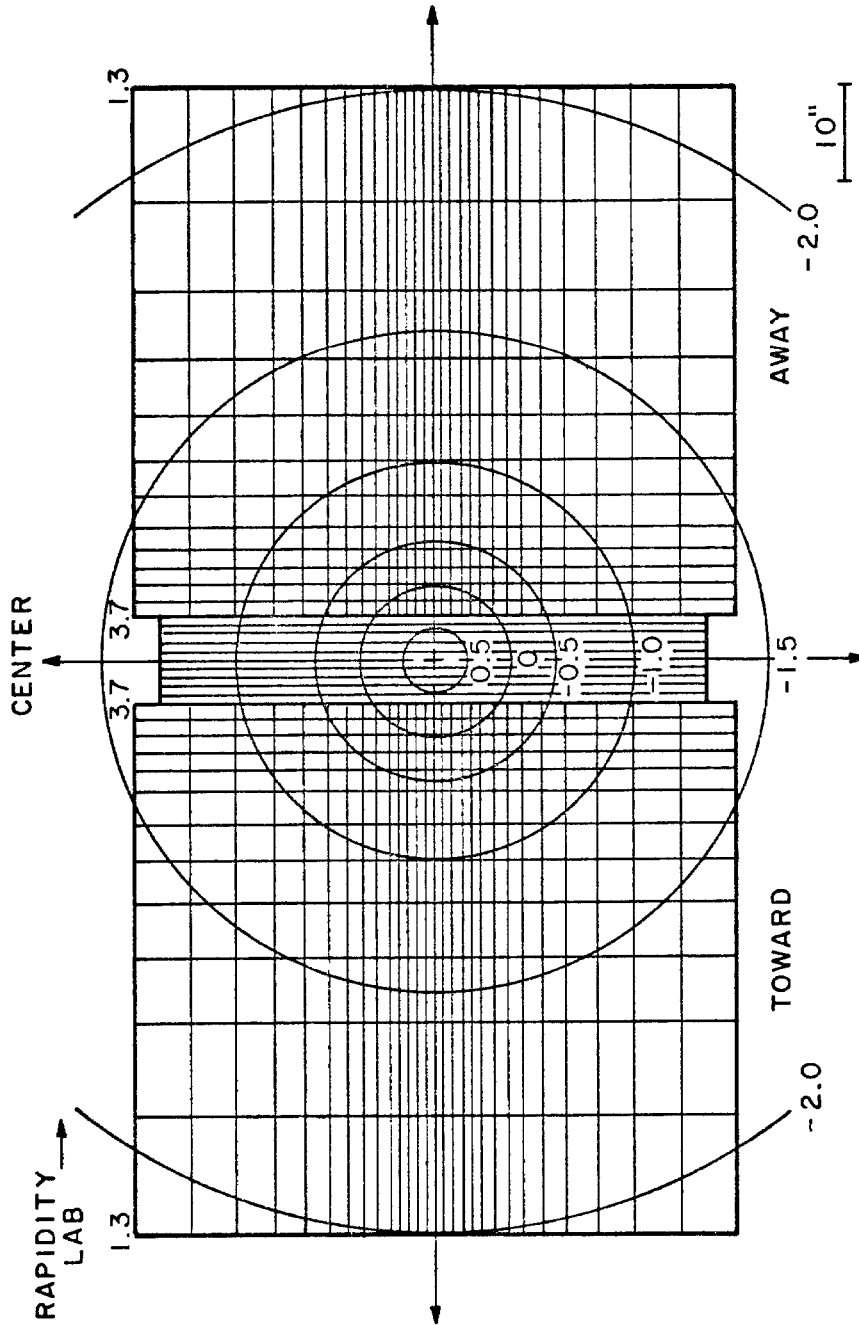


figure 4.

CROSS SECTIONAL VIEW AT 102" FROM TARGET



CALORIMETER DIVISIONS ARE IN 0.2 UNITS OF RAPIDITY IN THE LAB FOR "TOWARD" AND "AWAY" SECTIONS

figure 5.

SIMPLIFIED SIDE VIEW OF CALORIMETER

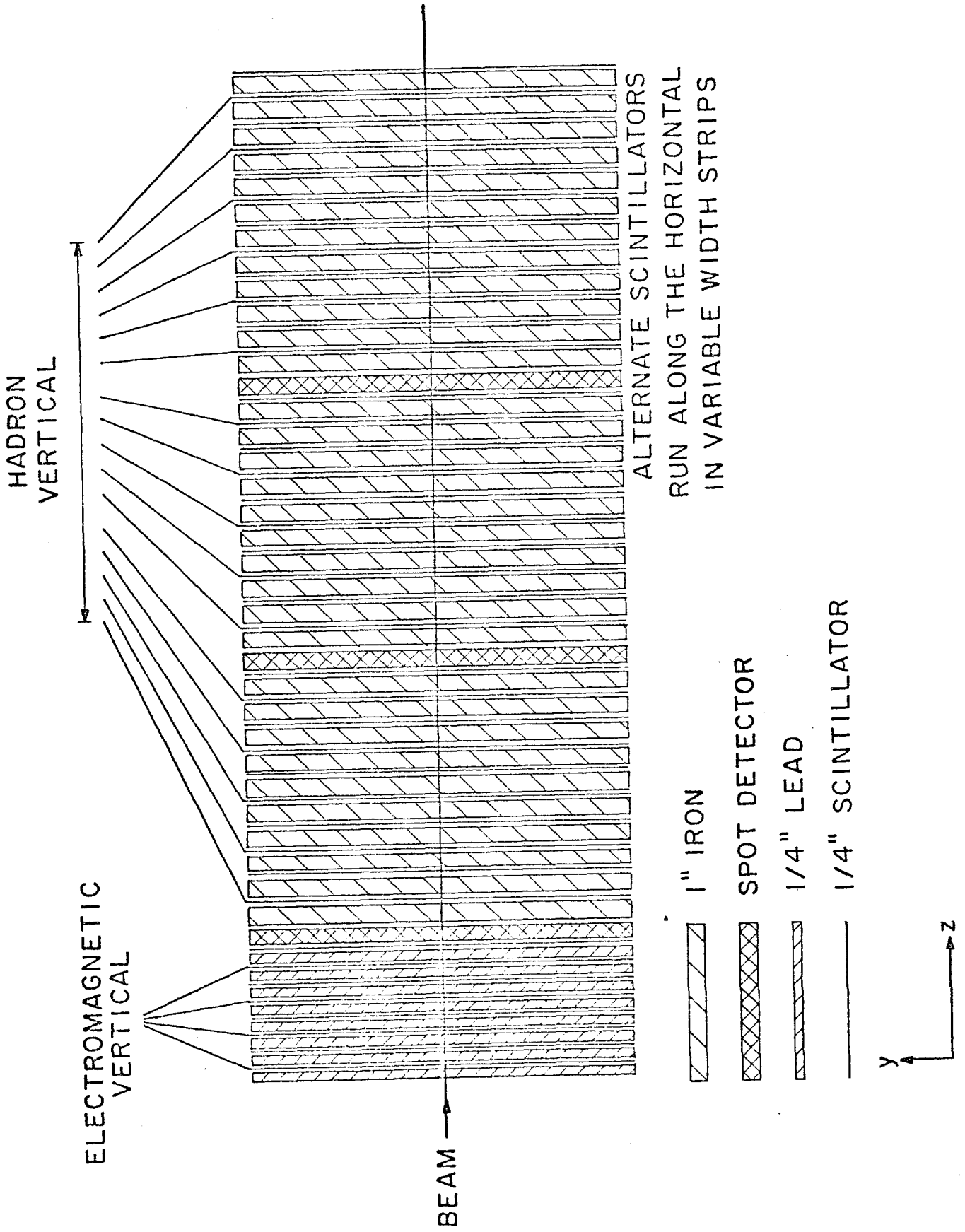


figure 6.

CMS POLAR ANGLE ACCEPTANCE

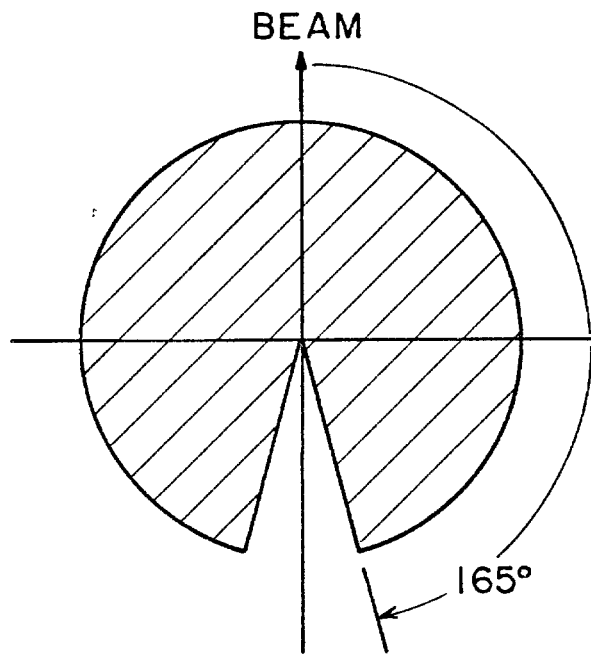


figure 7.

AVERAGE POSITION OF
SINGLE PARTICLE

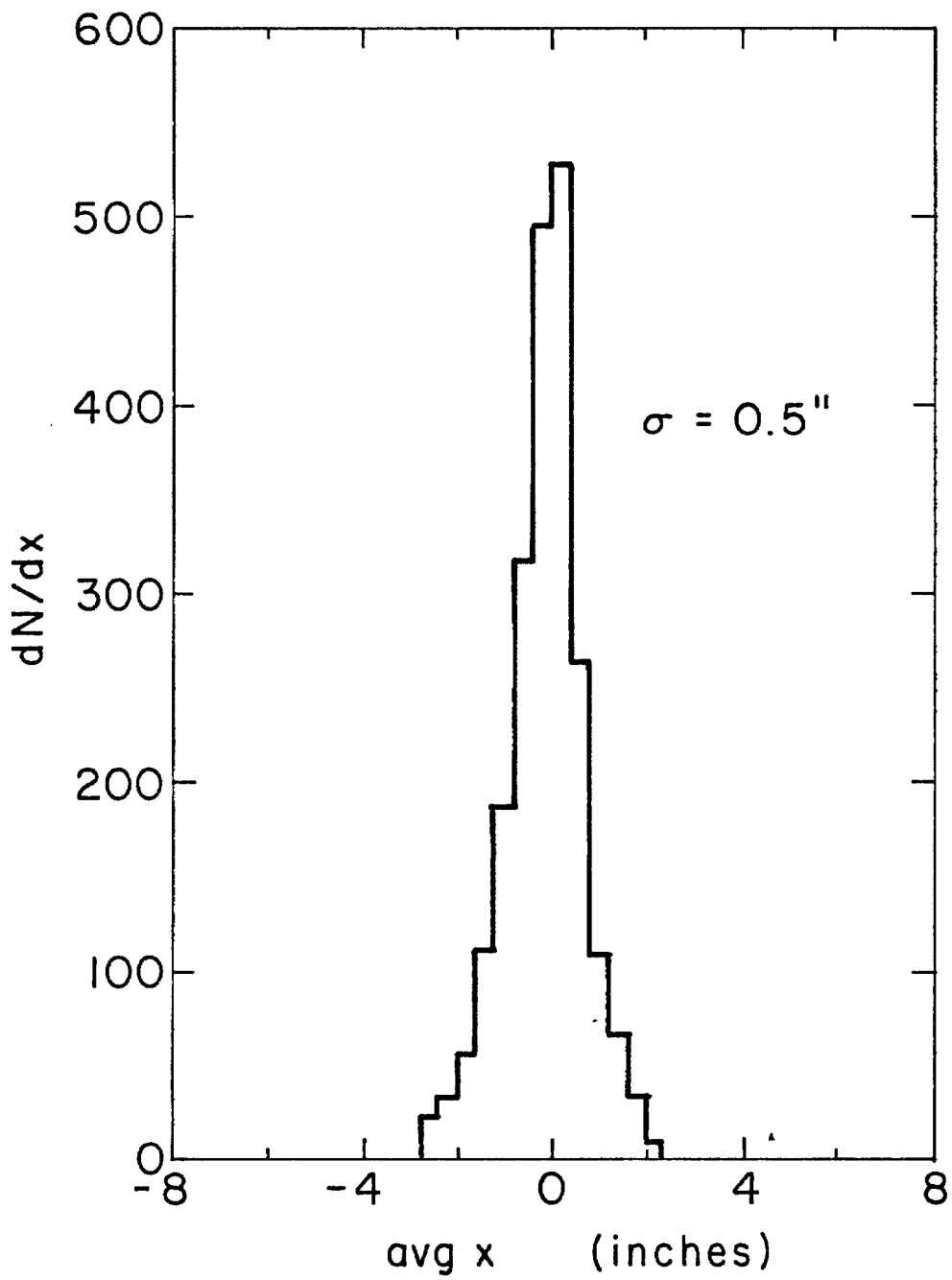


figure 8.

Figure 9

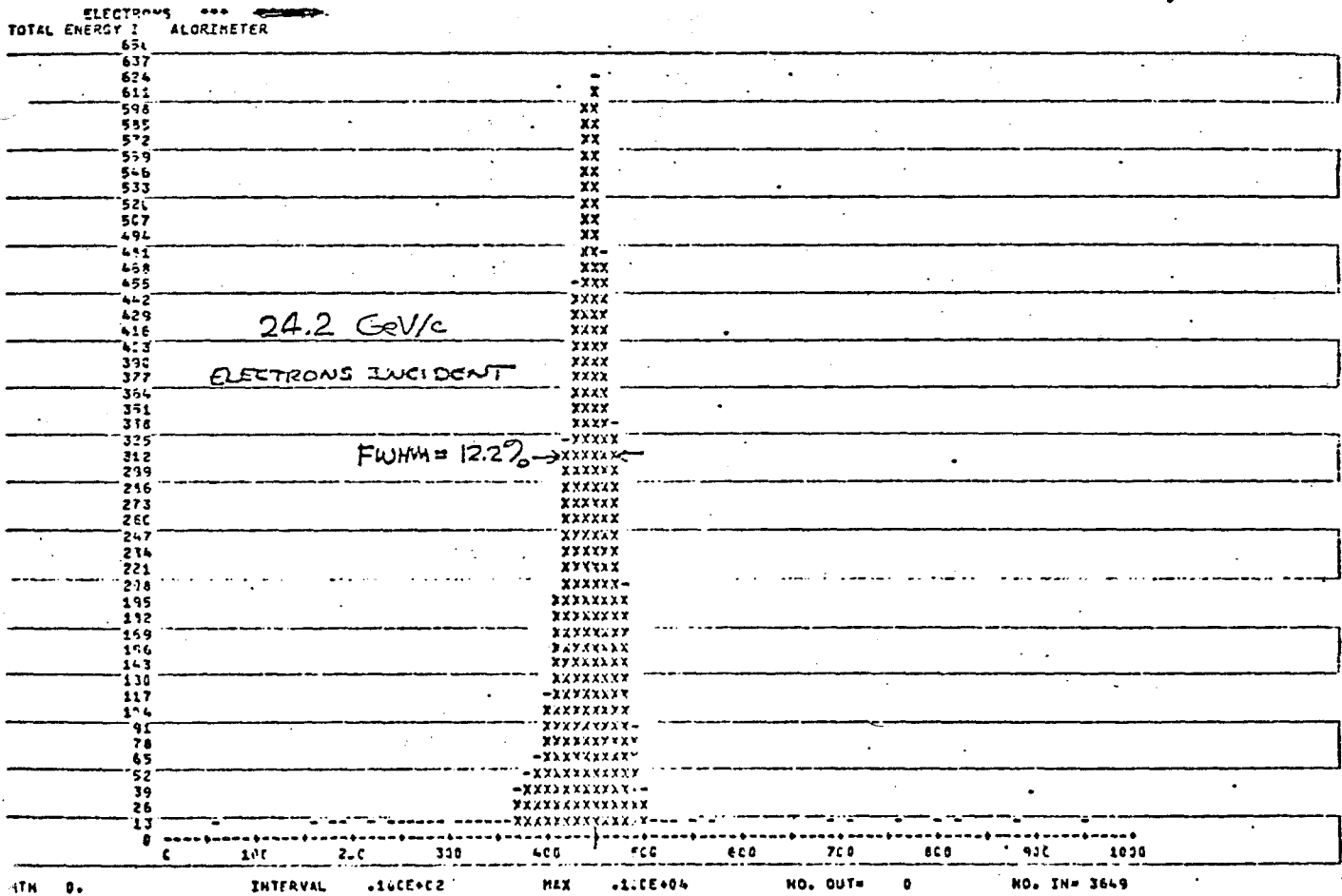
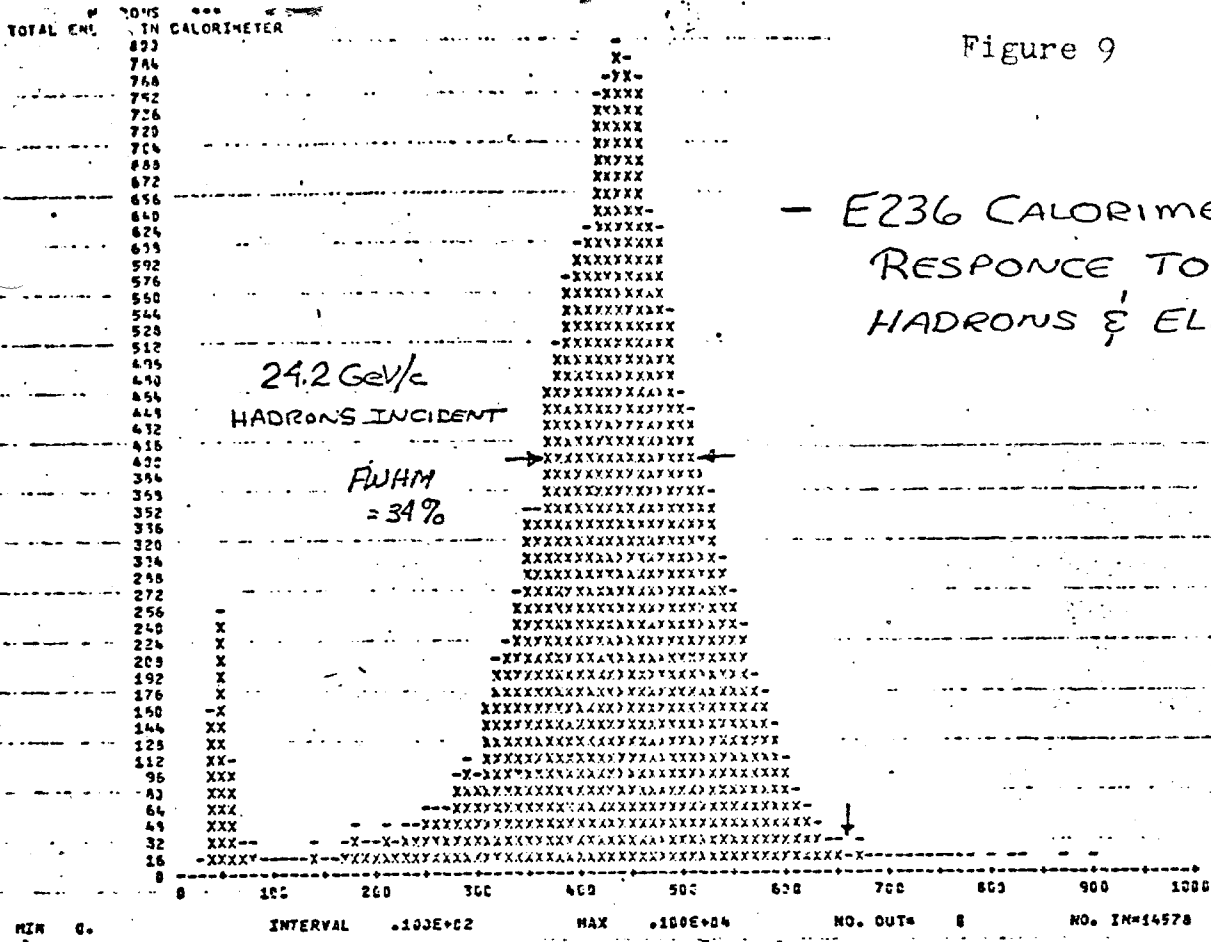


Figure 10
 Energy resolution as a function of incident
 energy of hadrons

.600
 .500
 $\frac{FWHM}{E}$
 .300
 .200
 .100

$$\frac{\Delta E \text{ (FWHM)}}{E} = \frac{1.2}{\sqrt{E}} + 0.09$$

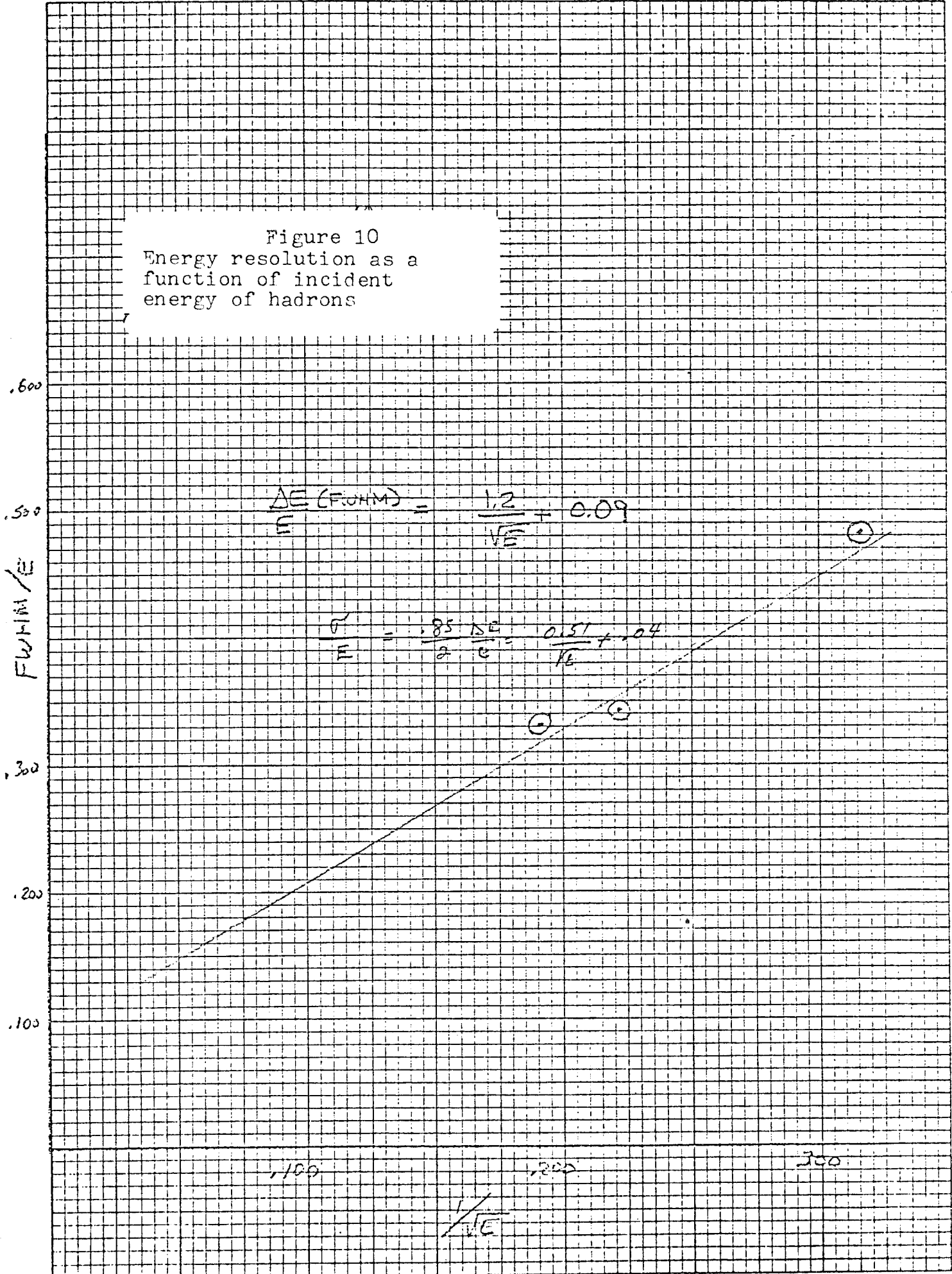
$$\frac{\sigma}{E} = \frac{.85}{2} \frac{\Delta E}{E} = \frac{0.51}{\sqrt{E}} + .04$$

100

200

300

$\frac{1}{\sqrt{E}}$

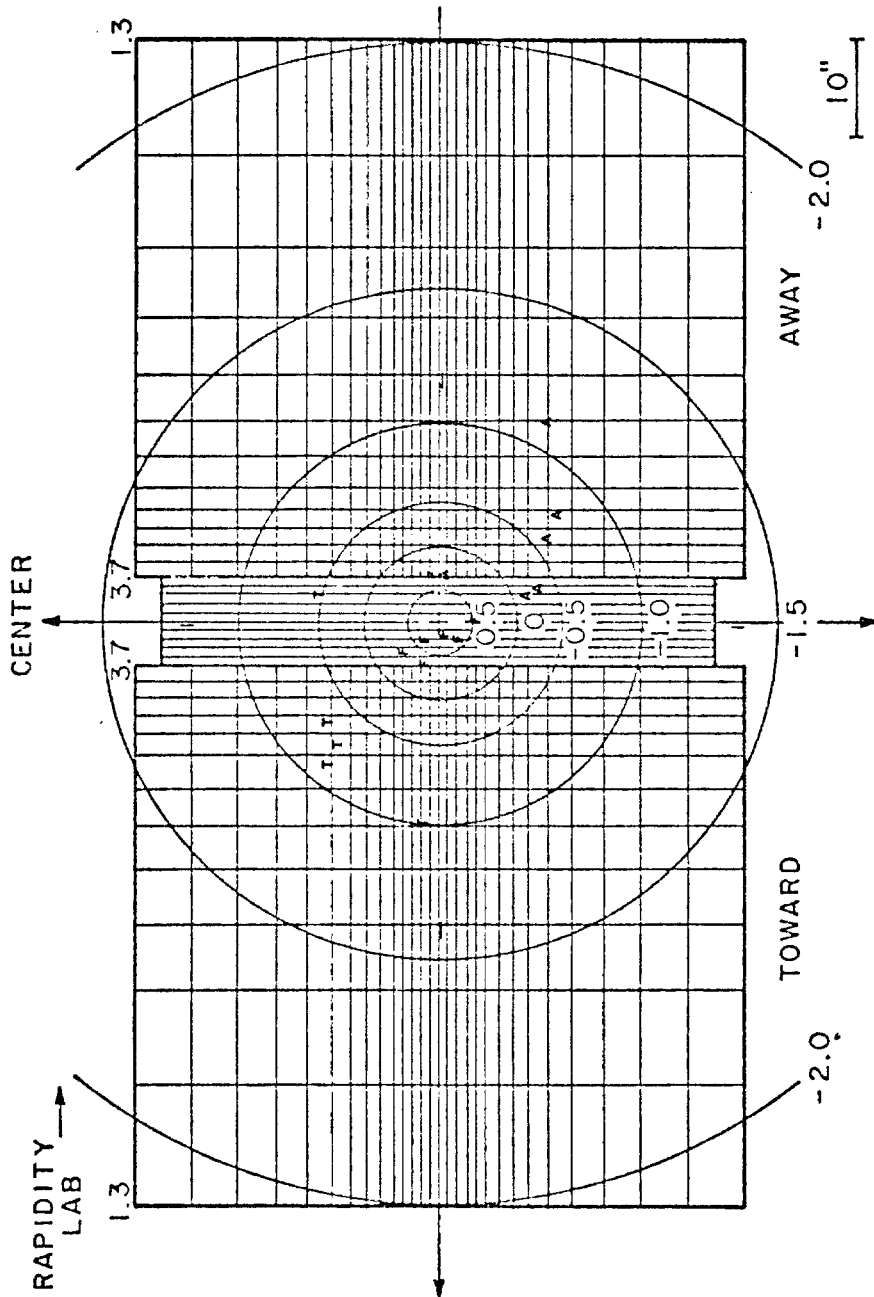


Calorimeter response as
a function of incident
hadron energy.

Figure 11.



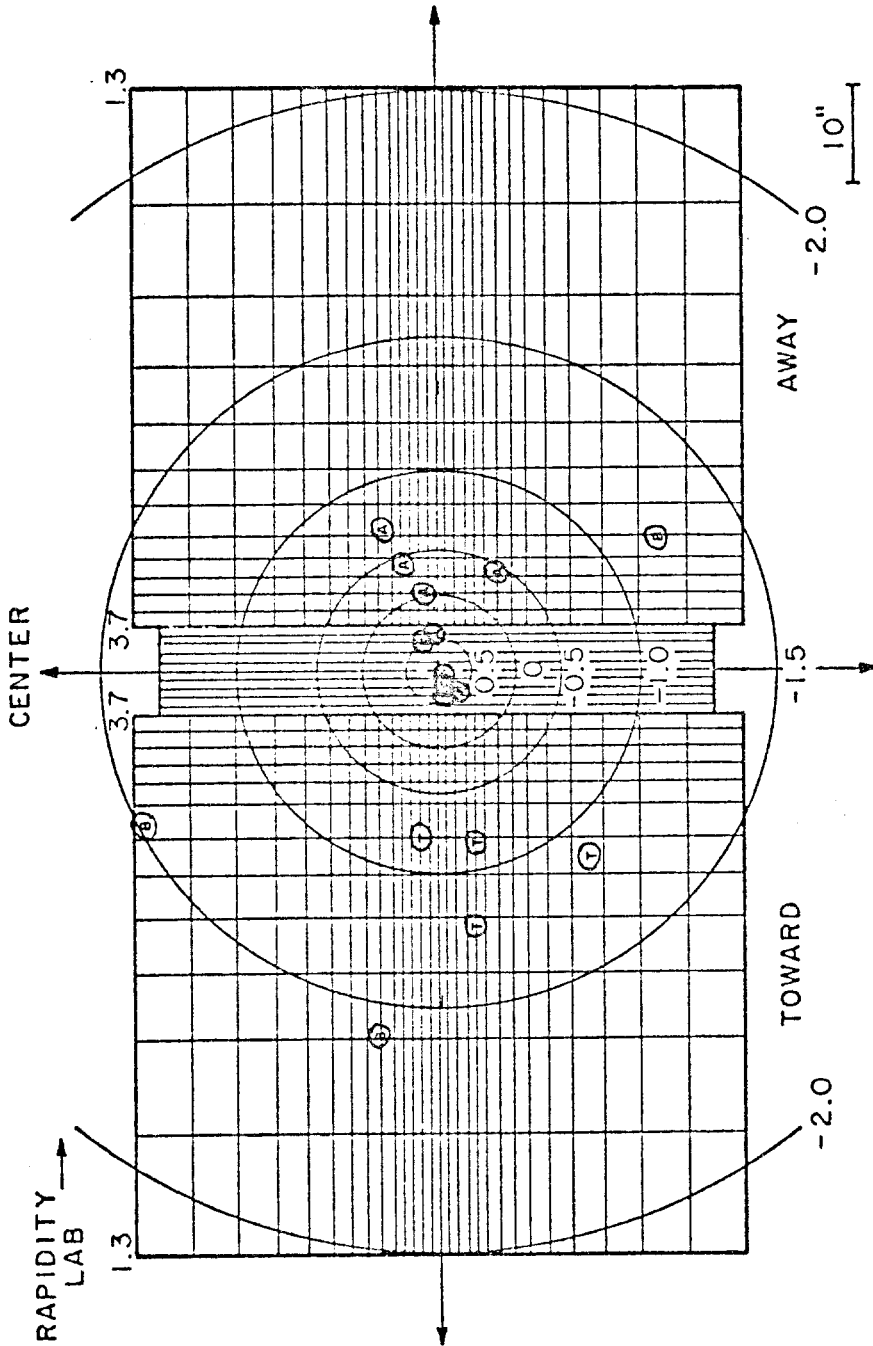
CROSS SECTIONAL VIEW AT 102" FROM TARGET



CALORIMETER DIVISIONS ARE IN 0.2 UNITS OF RAPIDITY
IN THE LAB FOR "TOWARD" AND "AWAY" SECTIONS

figure 12(a)

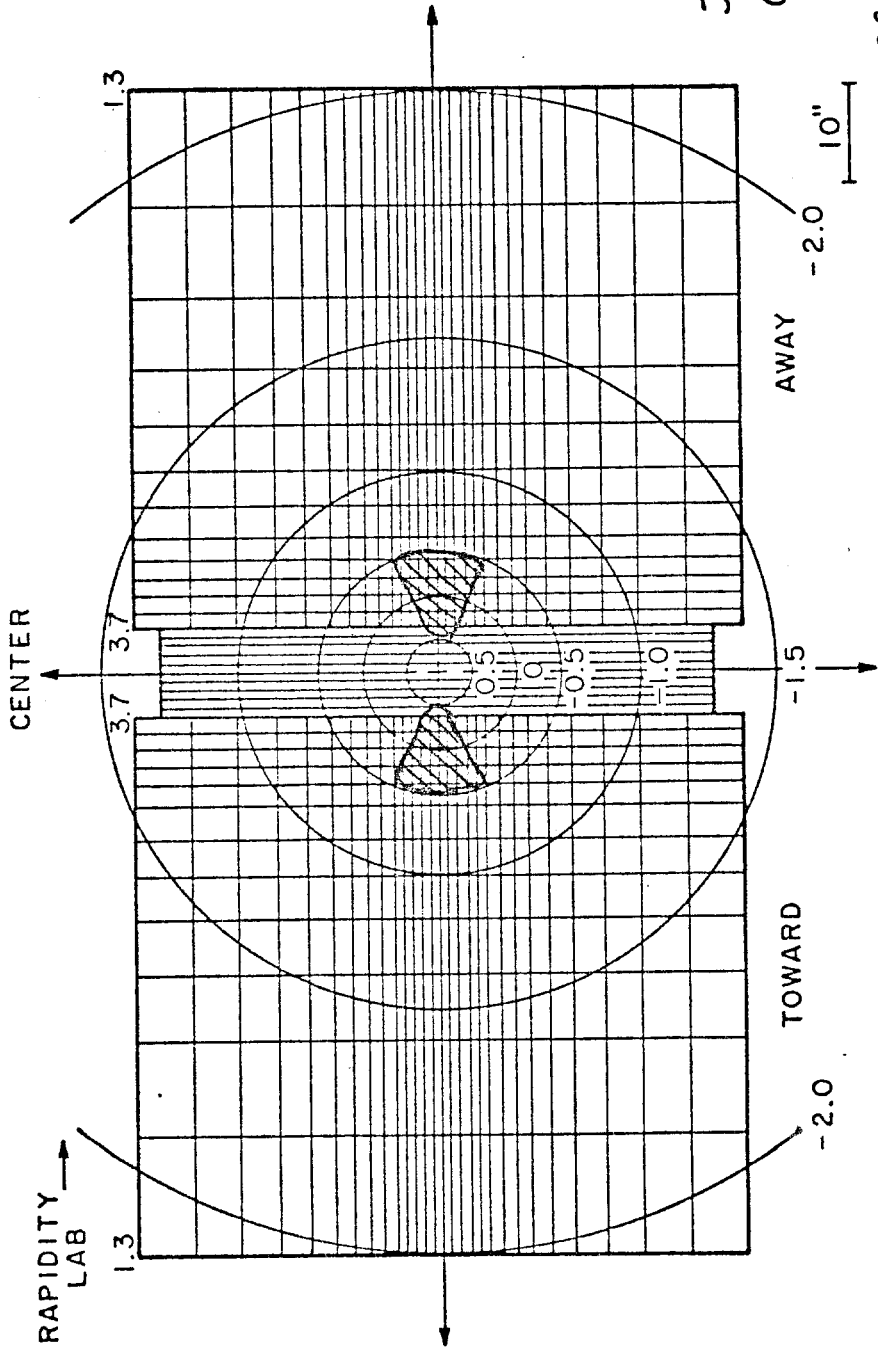
CROSS SECTIONAL VIEW AT 102" FROM TARGET



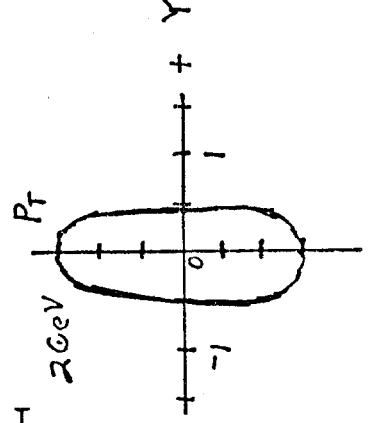
CALORIMETER DIVISIONS ARE IN 0.2 UNITS OF RAPIDITY IN THE LAB FOR "TOWARD" AND "AWAY" SECTIONS

figure 13.

CROSS SECTIONAL VIEW AT 102" FROM TARGET



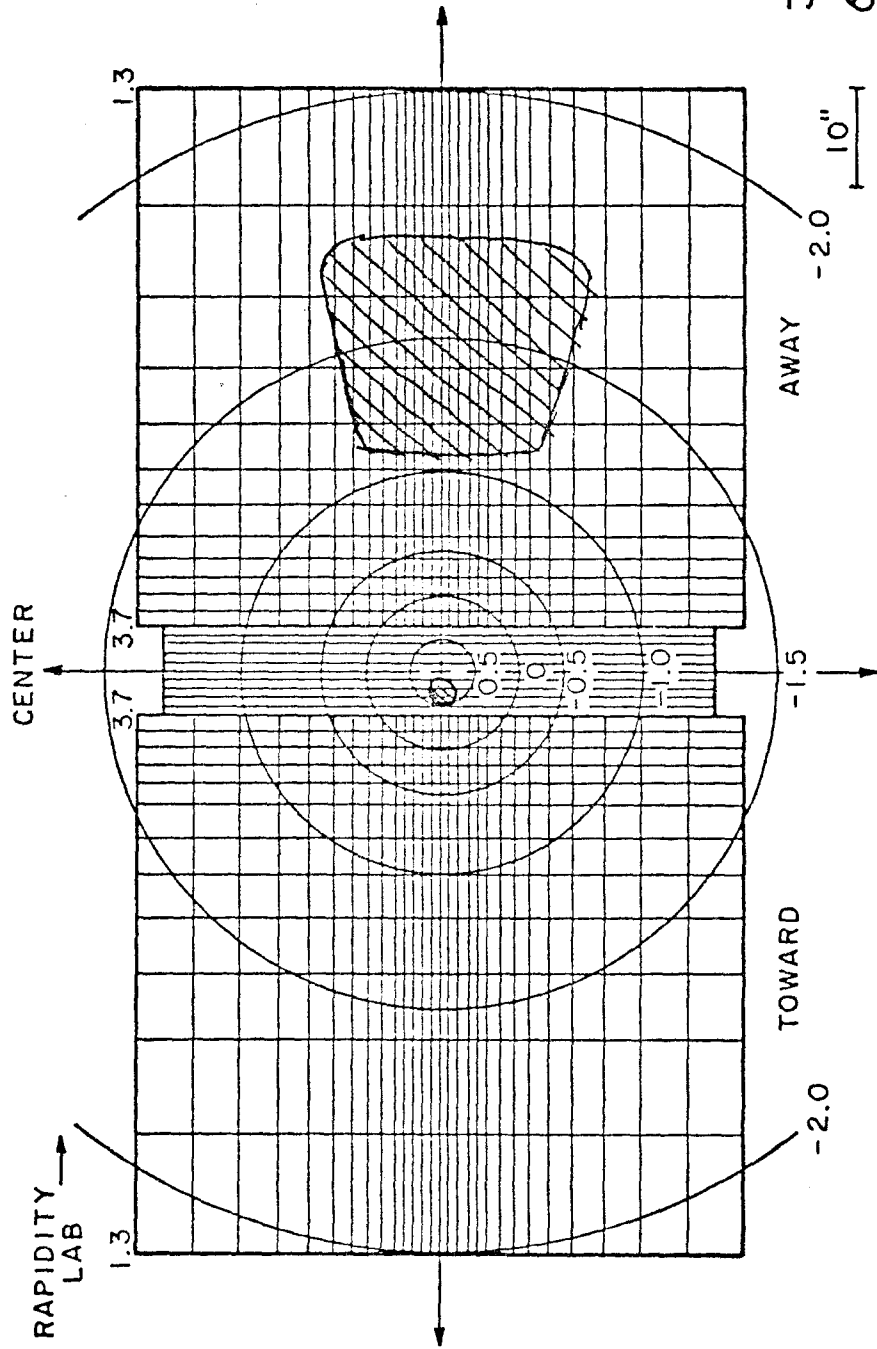
Jet-Jet
 $\Theta^* = 90^\circ$



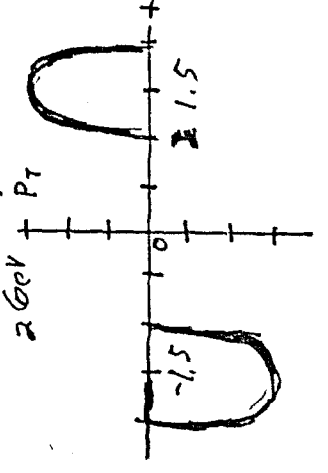
CALORIMETER DIVISIONS ARE IN 0.2 UNITS OF RAPIDITY
 IN THE LAB FOR "TOWARD" AND "AWAY" SECTIONS

figure 14(a)

CROSS SECTIONAL VIEW AT 102" FROM TARGET



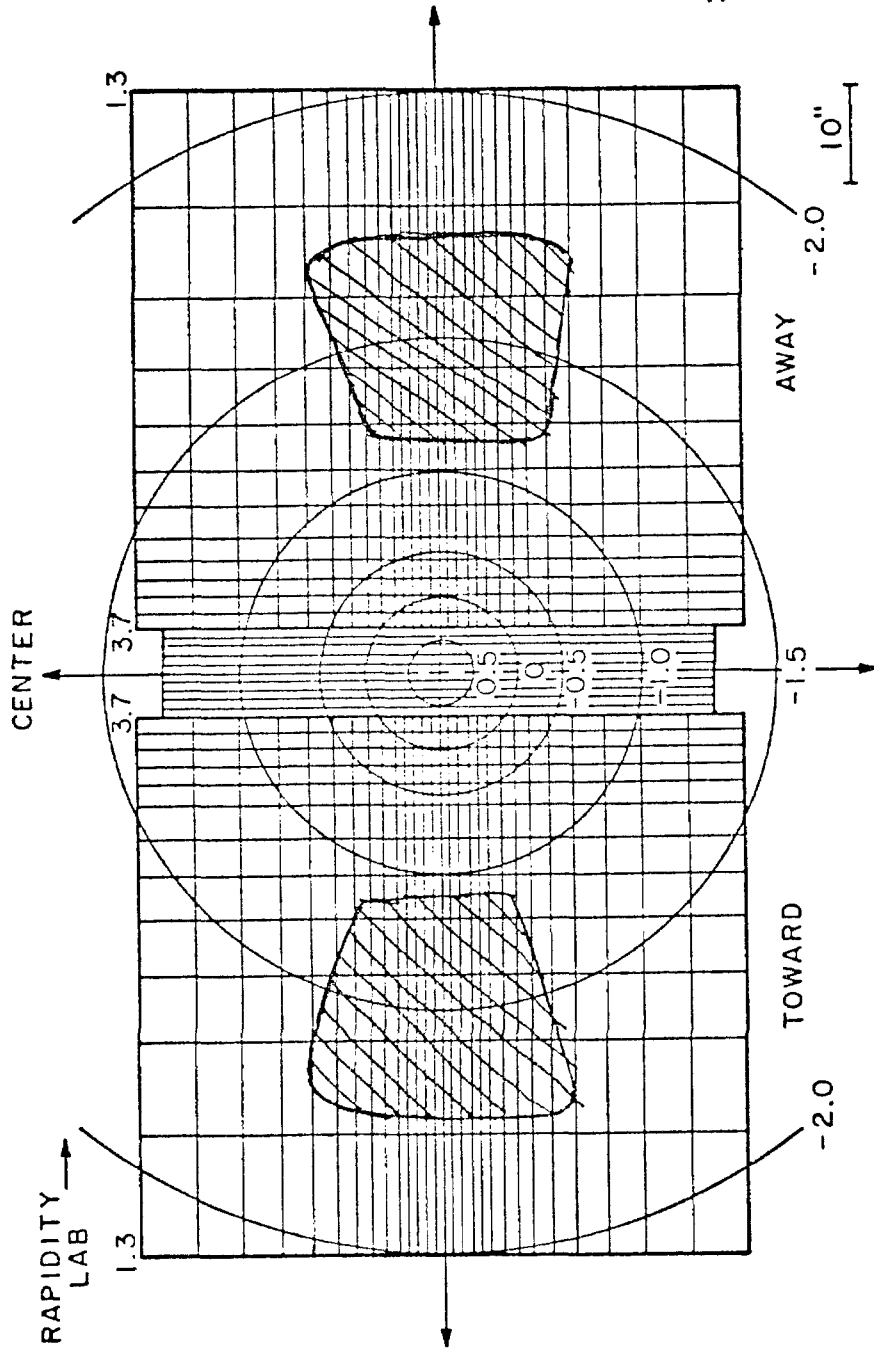
Jet - Jet
 $\theta^* = 40^\circ$
 $\frac{2\theta_{jet}}{P_T}$



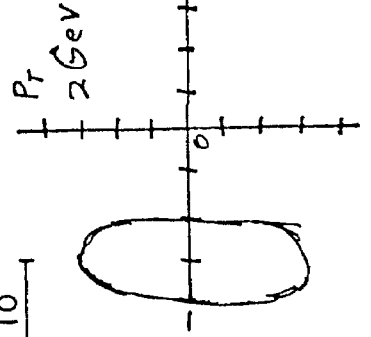
CALORIMETER DIVISIONS ARE IN 0.2 UNITS OF RAPIDITY
 IN THE LAB FOR "TOWARD" AND "AWAY" SECTIONS

figure 14(b)

CROSS SECTIONAL VIEW AT 102" FROM TARGET



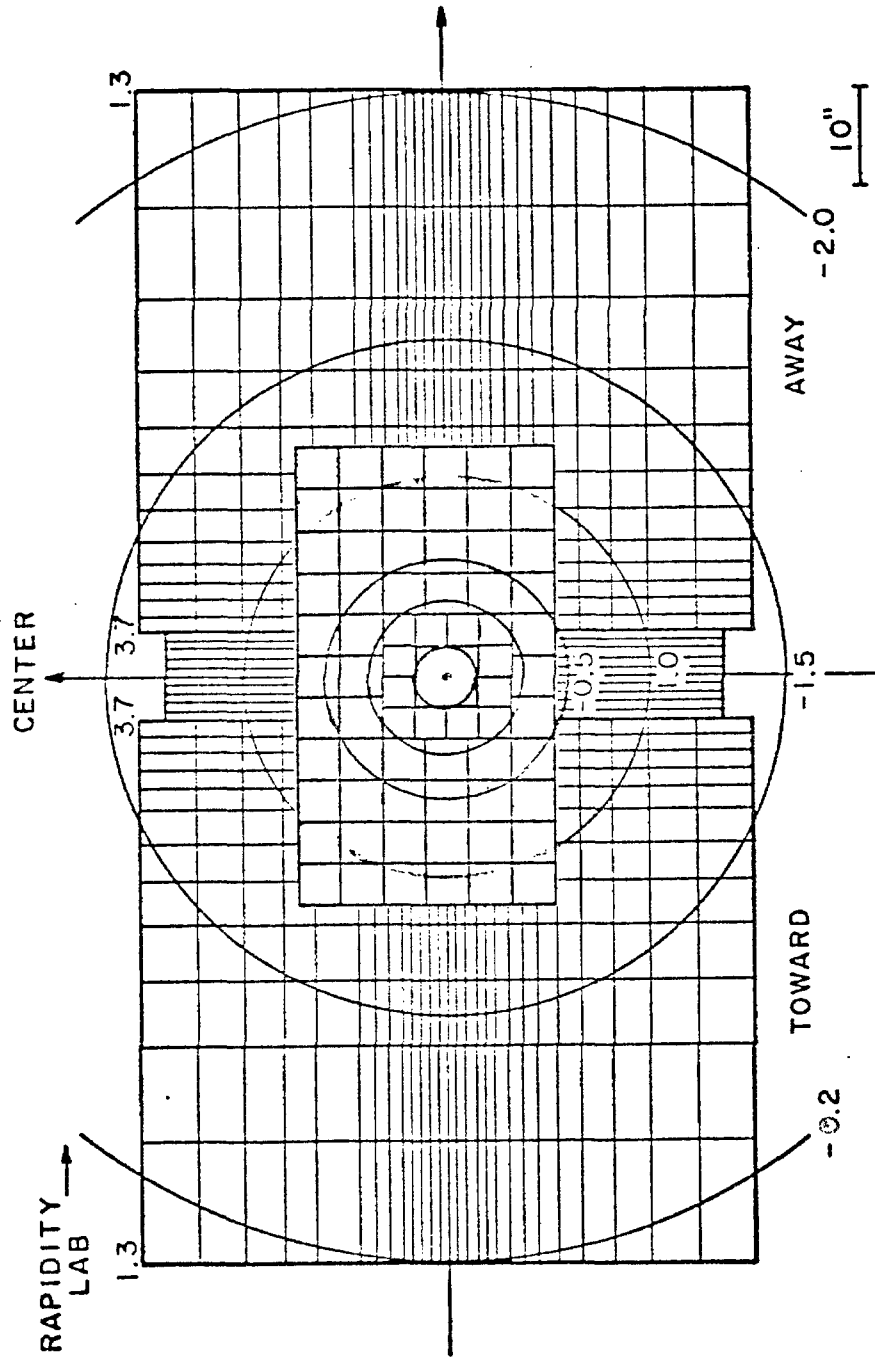
Jet - Jet



CALORIMETER DIVISIONS ARE IN 0.2 UNITS OF RAPIDITY IN THE LAB FOR "TOWARD" AND "AWAY" SECTIONS

figure 14(c)

CROSS SECTIONAL VIEW AT 102" FROM TARGET



CALORIMETER DIVISIONS ARE IN 0.2 UNITS OF RAPIDITY
IN THE LAB FOR "TOWARD" AND "AWAY" SECTIONS

figure 15.